



1

2

3

4

5

6

7

8

9

10

11

12

13

14

15

16

17

18

19

20

21

22

23

24

25

26

27

28

29

30

31

32

33

# Apportioning aerosol natural and anthropogenic sources thorough simultaneous aerosol size distributions and chemical composition in the European high Arctic

**Manuel Dall'Osto<sup>1\*</sup>, David C.S. Beddows<sup>2</sup>,  
Peter Tunved<sup>3</sup>, Roy. M. Harrison<sup>3†</sup>,  
Angelo Lupi<sup>4</sup>, Vito Vitale<sup>4</sup>,  
Silvia Becagli<sup>5</sup>, Rita Traversi<sup>5</sup>  
Ki-Tae Park<sup>6</sup> Young Jun Yoon<sup>6</sup>  
Andreas Massling<sup>7</sup>, Henrik Skov<sup>7</sup>  
Johan Strom<sup>2</sup> and Radovan Krejci<sup>2</sup>**

<sup>1</sup>Institute of Marine Science, Consejo Superior de Investigaciones Científicas (CSIC), Barcelona, Spain

<sup>2</sup>National Centre for Atmospheric Science Division of Environmental Health & Risk Management School of Geography, Earth & Environmental Sciences University of Birmingham, Edgbaston, Birmingham, B15 2TT United Kingdom

<sup>3</sup>Department of Environmental Science and Analytical Chemistry & Bolin Centre for Climate Research, Stockholm University, Stockholm 10691, Sweden

<sup>4</sup>Department of Chemistry, University of Florence, Via della Lastruccia 3, 50019, Sesto Fiorentino, Florence, Italy

<sup>5</sup>Institute of Atmospheric Sciences and Climate (CNR-ISAC), 40129 Bologna, Italy

<sup>6</sup>Korean Polar Research Institute, KOPRI, Republic of South Korea

<sup>7</sup>Arctic Research Centre, iClimate, Department of Environmental Science, Aarhus University, Roskilde 4000, Denmark

---

\* To whom correspondence should be addressed. Email: [dallosto@icm.csic.es](mailto:dallosto@icm.csic.es)

†Also at: Department of Environmental Sciences / Center of Excellence in Environmental Studies, King Abdulaziz University, PO Box 80203, Jeddah, 21589, Saudi Arabia



## 1 **ABSTRACT**

2 Understanding aerosol size distributions is crucial to our ability to predict aerosol number  
3 concentrations. When of favourable size and composition, both long range transported  
4 particles as well as locally formed ones may serve as Cloud Condensation Nuclei (CCN);  
5 small changes may have a large impact on the low CCN concentrations currently  
6 characteristic of the Arctic environment. Here, we present a cluster analysis of particle size  
7 distributions (PSD, size range 8-500nm) simultaneously collected from three high Arctic  
8 sites across Europe during a three year period (2013-2015). Two sites are located in the  
9 Svalbard archipelago: Zeppelin research station (474m above ground), and the nearby  
10 Gruvebadet Observatory (about 2Km distance from Zeppelin, 67m above ground). The  
11 third site (Villum Research Station – Station Nord, 30m above ground) is 600 km to the  
12 west-northwest of Zeppelin, at the tip of north-eastern Greenland. An inter-site comparison  
13 exercise is carried out for the first time including the Gruvebadet site. K-means analysis  
14 provided eight specific aerosol categories, further combined into broad PSD with similar  
15 characteristics, namely: pristine low concentrations (12-14%), new particle formation (16-  
16 32%), Aitken (21-35%) and accumulation (20-50%). Confined for longer time periods by  
17 consolidated pack sea ice regions, the Greenland site shows PSD with lower ultrafine  
18 mode aerosol concentrations during summer, but higher accumulation mode aerosol  
19 concentrations during winter relative to the Svalbard sites. By association with chemical  
20 composition and Cloud Condensation Nuclei properties, further conclusions can be  
21 derived. Three distinct types of accumulation mode aerosol are observed during winter  
22 months, associated with sea spray (largest detectable sizes), Arctic haze (main mode at  
23 150nm) and aged accumulation mode (main mode at 220nm) aerosols. In contrast, locally  
24 produced and most likely of marine biogenic origin particles exhibit size distributions  
25 dominated by the nucleation and Aitken mode aerosol during summer months. The



1 obtained data and analysis set now the stage for future studies; including apportioning the  
2 relative contribution of primary and secondary aerosol formation processes to the aerosol  
3 size distribution in high Arctic, and elucidating anthropogenic aerosol dynamics, transport  
4 and removal processes across the Greenland sea. In a region of enormous importance for  
5 future climate on Earth, it is imperative to continue strengthening international scientific  
6 cooperation, in order to address important research questions on scales beyond singular  
7 station or measurement events.

8

## 9 **1. INTRODUCTION**

10 The Arctic is a sensitive region affected by perturbations of the radiation budget, with  
11 complex feedback mechanisms resulting in a temperature increasing more than twice the  
12 global average since the 1980s (so-called “Arctic amplification”, Cohen et al., 2014, Pithan  
13 and Mauritsen, 2014). Aerosols are able to perturb the radiation balance of the Arctic  
14 environment in numerous ways (Carslaw et al., 2013). The contribution by aerosols to  
15 radiative forcing is considered a very important parameter, although still highly uncertain in  
16 a recent climate assessment (IPCC, 2014). In order to improve our knowledge in  
17 estimating direct and indirect climate effects, a better knowledge of the aerosols is an  
18 essential requisite, including their properties and seasonal variability, their sources, and  
19 the associated atmospheric reactions and transport processes. One of the main basic  
20 properties to characterize an aerosol is the size distribution. Atmospheric aerosol particles  
21 span over several orders of magnitude in diameter ( $D_p$ ), from a few nanometer to  
22 hundreds of micrometers. Small particles, in particular nucleation mode (typically with  $D_p$   
23  $<10$  nm) and Aitken mode ( $10 \text{ nm} < D_p < 100 \text{ nm}$ ) particles contribute little to total particulate  
24 mass in background air; however, they contribute significantly to surface area and



1 dominate particle number concentration (Dall’Osto et al., 2011). Measurements of Arctic  
2 aerosols have shown a strong annual cycle. The first full year of aerosol size distribution  
3 and chemical composition Arctic measurements was conducted at the Zeppelin station on  
4 Svalbard (Strom et al. 2003), showing a very strong seasonal dependence of the number  
5 mode particle size. Tunved et al. (2013) subsequently reported a qualitative and  
6 quantitative assessment of more than 10 yr of aerosol number size distribution data  
7 observed in the Arctic environment (Mt. Zeppelin, Svalbard); reporting that seasonal  
8 variation seems to be controlled by both dominant sources as well as meteorological  
9 conditions. This can be broadly summarised in three distinctly different periods:  
10 accumulation mode aerosol during the haze period (March–May), followed by a high  
11 concentration of small particles locally formed (June–August), leaving the rest of the year  
12 with a low concentration of accumulation mode particles and negligible abundance of  
13 ultrafine particles (September–February). Additional results from multi-year measurements  
14 reported similar conclusions using aerosol number size distributions collected at Tiksi  
15 (Asmi et al., 2016), Alert (Croft et al., 2016), Barrow (Latham et al., 2013) and Villum  
16 Research Station - Station Nord (Nguyen et al., 2016).

17 Currently, the Arctic haze is not well represented within atmospheric models, mainly due  
18 to inadequate representation of scavenging processes different transport mechanisms and  
19 underestimation and an unknown number of aerosol sources. As regards natural aerosol  
20 sources, they have been emphasized to be much more important than transport from  
21 continental sources. Recently, the aerosol population was categorised via cluster analysis  
22 of aerosol size distributions taken at Mt Zeppelin (Svalbard, Dall’Osto et al., 2017a) during  
23 an 11 year record (2000-2010) and at Station Nord (Greenland, Dall’Osto et al., 2018b)  
24 during a 7 year period (2010-2016). Air mass trajectory analysis linked these frequent  
25 nucleation events to biogenic precursors released by open water and melting sea ice



1 regions. Both studies reported a striking negative correlation ( $r = -0.89$  and  $-0.75$ ,  
2 respectively) between sea ice extent and nucleation events. Given the likely decrease in  
3 future sea ice extent in the Arctic, it is likely that the impact of natural ultrafine Arctic  
4 aerosols will increase in future. However, it was stressed that further studies are needed  
5 given other new particle formation source regions and mechanisms exist, including an  
6 influence of emissions from seabird colonies (Croft et al., 2016; Weber et al., 1998) and  
7 intertidal zones (O'Dowd et al., 2002; Sipila et al., 2016).

8 It is becoming evident that coordinated field measurement studies of the atmospheric size  
9 distribution of aerosols are essential to elucidate the complex interactions between the  
10 cryosphere, atmosphere, ocean, and biosphere in different regions (Dall'Osto et al., 2018  
11 a, b). In this regard, an emerging multi-year set of observed aerosol number size  
12 distributions in the diameter range of 10 to 500 nm from five sites around the Arctic Ocean  
13 (Alert, Villum Research Station – Station Nord, Zeppelin, Tiksi and Barrow) was recently  
14 assembled and analysed (Freud et al., 2017). Major accumulation mode aerosol sources  
15 were found over central Siberia and western Russia, and wet removal by snow or rain was  
16 found to be the main sink for accumulation-mode particles. It was argued that there is no  
17 single site that can be considered as fully representative for the entire Arctic region with  
18 respect to aerosol number concentrations and distributions. Following the pioneering study  
19 of Freud et al. (2017), the aim of this paper is to present a detail analysis of the main  
20 differences and similarities of the aerosol general features of the number size distributions  
21 between three different sites across the Arctic in the North Atlantic sector. Here, we use  
22 the stations named Gruebadet (GRU), Zeppelin (ZEP) and Villum Research Station –  
23 Station Nord (VRS). The European Arctic is understood here as the part of the circumpolar  
24 Arctic located between Greenland and northwest Russia. Geographically, Greenland is  
25 part of the continent of North America. However, the island is politically and culturally



1 associated with Europe (specifically with Norway, Denmark, as well as the nearby island of  
2 Iceland). In between Greenland and Svalbard there is the Fram Strait - located roughly  
3 between 77°N and 81°N latitudes and centered on the prime meridian - the only deep-  
4 water connection between the World Oceans and the Arctic. It is important to stress that  
5 the Svalbard archipelago is among the Arctic regions that has experienced the greatest  
6 temperature increase during the last three decades (Nordli et al., 2014); therefore  
7 comparing aerosol measurements simultaneously collected in Greenland and Svalbard is  
8 essential to better understand aerosol sources and processes that may affect our  
9 changing climate. Previous studies have focused on the characterization via air mass  
10 origin frequency and occurrence of different aerosol modes over time scales of the order of  
11 periods of weeks to years (Strom et al., 2003; Tunved et al., 2010; Nguyen et al., 2016;  
12 Lupi et al., 2016), but only using a single station as monitoring site. A brief comparison  
13 between ZEP and GRU was made in Lupi et al (2016), showing good agreement over a  
14 period of three months. However, to capture all scales of the variability of Arctic aerosols,  
15 it is important to merge intensive field campaigns and long-term measurements across  
16 different stations. Provision of the extensive resource-demanding equipment required is  
17 only possible by means of international collaborations such those created in the present  
18 work. A growing effort in understanding recent drastic changes in the Arctic climate has  
19 stimulated more measurements, and a growing number of monitoring sites and  
20 atmospheric measurements are taking place. Freud et al. (2017) for the first time  
21 assembled and analysed a multi-year set of observed aerosol number size distributions in  
22 the diameter range of 10 to 500 nm from five sites around the Arctic Ocean (Alert, Villum  
23 Research Station – Station Nord, Zeppelin, Tiksi and Barrow). Here, aerosol size  
24 distributions are analyzed by using k-means cluster analysis (Beddows et al., 2009)  
25 applied to a long term dataset composed of three years (2013-2015) simultaneous data



1 from three stations (GRU, ZEP, VRS). This is the first time that the GRU site is used in a  
2 multi-year set of observed aerosol number size distributions. All size distributions are  
3 quality assured, and not filtered according to any other criteria. The cluster analysis herein  
4 applied uses the degree of similarity and difference between individual observations to  
5 define the groups and to assign group membership. By doing so, our clustering method  
6 provides a specific number of size distributions which can be compared across different  
7 time periods and across different monitoring sites (Beddows et al., 2009; Dall’Osto et al.,  
8 2018b). Whilst a number of intensive field studies have been focusing on single site  
9 datasets (Tunved et al., 2004; Dall’Osto et al., 2017a, Dall’Osto et al., 2018b), cluster  
10 analyses of multi-site year-long particle size distributions measurements are scarce (Freud  
11 et al., 2017; Dall’Osto et al., 2018b). It is important to stress in this study the only aim was  
12 to compare the three stations by apportioning different aerosol categories and possible  
13 source associations. Future studies will look at transport, both vertical (i.e. between VRS  
14 and GRU/VRS) and horizontal (i.e between GRU and ZEP) of both anthropogenic and  
15 natural aerosols.

16

## 17 **2. METHODS**

### 18 **2.1 Site Description**

19 Ultrafine aerosol size distributions were measured at three different sites. Fig. 1 (a,b)  
20 shows the location and the sea ice coverage across the whole of 2015 taken as an  
21 example.

22 The first measurement site is situated at 78° 580N and 11° 530E on the Zeppelin Mountain  
23 in the Ny-Alesund community on Svalbard. The Zeppelin (ZEP) station is located 474m  
24 above sea level, it is easily accessible yet practically unaffected by local sources.



1 Compared to stations closer to sea level the Zeppelin station is less affected by local  
2 particle production occurring in the surf zone, and to local air flow phenomena such as  
3 katabatic winds (Strom et al., 2003). The ZEP station is part of ACTRIS Data Centre  
4 (ACTRIS DC, developed through the EU project Aerosols, Clouds, and Trace gases  
5 Research InfraStructure Network - URI: <http://www.actris.eu> - within the EC 7th  
6 Framework Programme under "Research Infrastructures for Atmospheric Research"), part  
7 of the Global Atmosphere Watch (GAW) programme; and it is likely the longest Arctic  
8 aerosol size distribution dataset existing (Strom et al., 2003, Tunved et al., 2010; Freud et  
9 al., 2017).

10 The Gruebadet (GRU) observatory is located in the proximity of the village of Ny-Alesund  
11 (78° 55 N, 11° 56 E) in the island archipelago of Svalbard. The observatory is 67 m above  
12 sea level, located south-east of the main buildings of the village. The instrument collected  
13 aerosol size distribution usually from the end of March to the beginning of September. It is  
14 located at about 2Km distant from the ZEP station, at about 350m lower altitude.

15 About 800Km away from Svalbard we have the Station Nord Villum research station  
16 (VRS). Located at 81° 36' N, 16° 40' W the station is situated in the most north-eastern  
17 part of Greenland, on the coast of the Fram Strait. The sampling took place about 2 km  
18 south-west of the main facilities of the Station Nord military camp in two different sampling  
19 stations as measurements were shifted in summer 2015 from the original hut called  
20 "Flygers hut" to the new air observatory, 300 m west of "Flygers hut". The sampling  
21 locations were located upwind from the station for most of the time. Detailed descriptions  
22 of the site and analysis of predominant wind directions are available elsewhere (Nguyen et  
23 al., 2016; Nguyen et al., 2013)

24



1 **2.2 Dataset**

2 **2.2.1 ZEP DMPS**

3 The Differential Mobility Particle Sizer (DMPS) system comprises a custom-built twin DMA  
4 (differential mobility analyser) setup including one Vienna-type medium DMA coupled to a  
5 TSI CPC 3010 covering sizes between 25 and 800 nm and a Vienna-type short DMA  
6 coupled with a TSI CPC 3772, effectively covering sizes between 5 and 60 nm. The  
7 number size distributions from the two systems are transferred to a common size grid and  
8 then merged. Both systems use a closed-loop setup. The instrument has been inter-  
9 calibrated during an ACTRIS ([www.actris.eu](http://www.actris.eu)) workshop. Sizing and number concentrations  
10 are within 1 and 5% from the standard DMPS, respectively (Freud et al., 2017).

11

12 **2.2.2 GRU SMPS**

13 Aerosol size distribution in the diameter range from 10.4 to 469.8 nm using 54 channels  
14 was evaluated with a commercial Scanning Mobility Particle Sizer SMPS TSI 3034,  
15 (Hogrefe et al. 2006), with a time resolution of 10 min and particle size with a resolution of  
16  $d \log D_j$  equivalent to 0.0312, where  $D_j$  indicates the instrumental class size. Further  
17 information can be found elsewhere (Lupi et al., 2016).

18 **2.2.3 VRS SMPS**

19 Scanning Mobility Particle Sizer (SMPS) data were collected in the period 2013-2015 in  
20 the size range of 9-915 nm in diameter. The SMPS used either a condensation particle  
21 counter (CPC) model TSI 3010 or model TSI 7220. To ensure correct functioning,  
22 volumetric flow rates, temperatures and relative humidity (RH) of the aerosol- and sheath  
23 flow were monitored, as well as inlet ambient pressure. No additional drying was



1 performed, as the transition from the low ambient temperatures outside of the huts (-45 to  
2 +15 °C, yearly average -15 °C) to the heated inside (>20 °C) generally provides sufficient  
3 decrease in RH.

4

### 5 **2.3 Data analysis and additional chemical and physical supporting data**

6 SMPS data from the three different stations were merged and only days where  
7 measurements were taken simultaneously at the three stations were considered in this  
8 analysis, resulting in 584 total days. Additional chemical and physical data were included  
9 in this study, in order to better describe the aerosol particle types sampled. PM<sub>10</sub> sampling  
10 was performed at GRU station by a TECORA Skypost sequential sampler equipped with a  
11 PM<sub>10</sub> sampling head operating following the EN 12341 European protocol. Aerosol  
12 samples were collected daily on Teflon (PALL Gelman) filters from March to September  
13 2013-2015, in total 385 daily samples were analysed. MSA was determined by ion  
14 chromatography on the aqueous extract obtained from one half of each filter (Becagli et  
15 al., 2016). Gaseous NH<sub>3</sub> and SO<sub>2</sub> data, and inorganic aerosol species (Na, Mg, Cl, K,  
16 sulphate, nitrate, ammonium) at the ZEP monitoring site were obtained at daily resolution  
17 at the NILU website data for the period 2013–2015 (total days 650). Concentrations of  
18 Cloud Condensation Nuclei (CCN) were measured continuously using a commercial  
19 available Droplet Measurement Technology (DMT) CCN counter at the ZEP station. In this  
20 study we selected CCN values when supersaturation is 0.4%. In total, 723 days of  
21 sampling were obtained at hourly resolution for the years 2013-2015. The size distribution  
22 data were averaged over 24 hours using the start and end time of the chemical  
23 measurements.

24



## 1 **3 RESULTS AND DISCUSSION**

2

### 3 **3.1 Average monthly size distributions**

4

5 The monthly averaged aerosol size distributions at the three sites are presented in Fig. 2.  
6 Simultaneously collected data are presented for the whole years (2013-2015), but only for  
7 8 months (March-October) considering all three sites, due to GRU not having data  
8 coverage during winter months (November through February). The average size  
9 distributions at ZEP and VRS are broadly similar during the months of January and  
10 February (2a-b), with low particle number concentrations and a broad accumulation mode,  
11 although larger at the ZEP site (about 250nm) than at the VRS one (about 180nm). The  
12 months of March and April (Fig. 2c-d) present similar size distributions among the three  
13 stations, showing a main large accumulation mode peak at about 190nm, likely associated  
14 with the Arctic haze occurring mainly during these months. It is worth noting that higher  
15 ultrafine particle number concentrations are seen in these two months relative to Jan-Feb  
16 (Fig. 2a-b). During the month of May (Fig. 2e) a clear increase of ultrafine particles can be  
17 seen at the Svalbard sites (GRU, ZEP) due to local new particle formation. The increased  
18 occurrence of new particle formation events (NPF) in May was found to correspond to the  
19 increasing concentration of biogenic aerosol in the Svalbard sites (Becagli et al., 2016;  
20 Dall'Osto et al., 2017a). Interestingly, the VRS site does not show this enrichment, likely  
21 due to the fact that sea ice is still covering most of the areas near the north-east corner of  
22 Greenland. In contrast, during the summer months of June-August, higher concentrations  
23 of ultrafine particles can be seen progressively at all sites. The changes in sources, sinks  
24 and processes associated with colder autumn months (Tunved et al., 2013; Freud et al.,  
25 2017) progressively shifts the aerosol modes seen at about 20-40nm (September, Fig. 2i)  
26 to a bimodal-like aerosol distribution seen in October (Fig. 2j) with two main aerosol modes



1 at about 50nm and 150nm, respectively. The remaining winter months show low particle  
2 number concentrations, and data are available for ZEP and VRS only. The data herein  
3 presented so far help us to compare the three monitoring sites. As expected, whilst the  
4 sites at GRU and ZEP are broadly similar, the VRS site located in Greenland seems to  
5 have fewer new particle events with a shorter summer frequency. In order to fully elucidate  
6 the chemical and physical processes affecting the aerosol size distributions, we use  
7 statistical tools to reduce the complexity of these SMPS datasets.

8

9

### 10 **3.2 K-means clustering analysis**

11

12

13 Approximately 25,000 aerosol size distributions obtained at one hour resolution at the  
14 three monitoring sites were averaged to daily resolution and then normalised by their  
15 vector-length and cluster analysed (Beddows et al., 2009). The standard procedure used  
16 (Beddows et al., 2014) including the Cluster Tendency test provided a calculated a  
17 Hopkins Index of 0.20 (Beddows et al., 2009). The method used minimize the sum of  
18 squared distances between all points and the cluster centre, allowing identification of  
19 homogeneous groups by minimizing the clustering error defined as the sum of the squared  
20 Euclidean distances between each dataset point and the corresponding cluster center.  
21 The complexity of the dataset is reduced allowing characterization of the data according to  
22 the temporal and spatial trends of the clusters. In order to choose the optimum number of  
23 clusters the Dunn-Index (DI) identified dense and well separated clusters, it provided a  
24 clear maximum for 8 clusters, some of which belonged only to specific times of the day,  
25 specific mechanisms as well as specific seasons. The eight K-means clusters obtained  
26 exhibited frequencies which varied between 1% and 42% (Table 1), without main clusters



1 dominating the overall population. The individual clusters could be distributed into three  
2 main groups named nucleation, Aitken and accumulation categories. This additional  
3 categorisation was based not only upon their similar size distributions among each other  
4 (see Fig. 3a–d) but also by considering strong similarities between other chemical and  
5 physical parameters presented in the next sections. The reduction to the three more-  
6 generic classifications was based on our data interpretation, and the average aerosol size  
7 distributions of each aerosol category are presented in Fig. 3: (a) pristine and nucleation  
8 mode particle types; (b) Aitken mode dominating particle type and (c) accumulation mode  
9 dominating particle type, and presented together in Fig. 3 (d).

10

### 11 **3.2.1 Aerosol categories and occurrence**

12

13 An aerosol K-means cluster can be interpreted as a particle size spectrum which is  
14 determined by a superposition of individual sources and processes. Therefore, the name  
15 associated with each cluster aims only to reflect a main feature associated with the particle  
16 size spectrum. It is not possible to associate a single source or process, given that each  
17 cluster results mainly from a combination of multiple sources. Fig. 3a (blue line) shows that  
18 the *pristine* category is associated with very low particle number concentrations (<100  
19 particles cm<sup>-3</sup>). Figure 3a shows average aerosol number concentrations across different  
20 sizes, with two minor modes at 35nm and 135nm. The *nucleation* category (Fig. 3a, red  
21 line) shows average daily aerosol number size distributions peaking in the smallest  
22 detectable size at 10nm. The name of this category - which will be used below to represent  
23 new particle formation events - stands for continuous gas-to-particle growth occurring after  
24 the particle nucleation event. By contrast, Figure 3a (green line) shows the average  
25 number size distribution with an ultrafine mode peaking at about 20-30nm. We refer this



1 *bursting* category to a population that bursts and begin to exist or develop. Contrary to the  
2 *nucleation* category, this one fails to grow to larger sizes. The origins of this particle type  
3 can be multiple, including new particle formation with limited growth (so called "apple" new  
4 particle formation events), or open ocean nucleation, an Arctic ultrafine primary origin can  
5 also not be ruled out.

6 Fig. 3b shows two main aerosol categories with a dominating aerosol mode peaking in the  
7 Aitken size range at about 40-60nm. Whilst aerosol category *nascent* possess a main  
8 mode at about 40nm, the category *nascent broad* shows a much broader Aitken mode  
9 peaking at about 60nm. By contrast, Fig. 3c shows three aerosol categories whose aerosol  
10 size distributions are all mainly distributed in size ranges larger than 100nm (accumulation  
11 mode dominating. Main modes can be seen at 150nm (category *accumulation\_150*), at  
12 220nm (category *accumulation\_220*) and in the largest detected modes at about 400-  
13 500nm (category *coarse*).

14 The temporal frequency during the years 2013-2015 of the eight aerosol categories is  
15 presented in Table 1. The category *pristine* presents a remarkably similar occurrence  
16 among the three monitoring sites (12-14%). The *nucleation* category seems more frequent  
17 at the Svalbard sites (11-15%) relative to the VRS site (8%). Similar patterns can be seen  
18 for the *bursting* category, also more frequent at GRU-ZEP (14-21%) relative to VRS (8%).  
19 Interestingly, the *bursting* shows high occurrence at GRU (21%), perhaps reflecting some  
20 processes occurring near sea level across the fiord. The two Aitken categories (*nascent*  
21 and *nascent broad*) do not show much variability (7-21%). By contrast, strong differences  
22 are seen in the accumulation dominating mode aerosol categories. For example,  
23 *accumulation\_150* is frequent at the ZEP site (19%), whereas at the VRS site the category  
24 dominating is *accumulation\_220* (42%), confirming a recent study specific on  
25 characterization of distinct Arctic aerosol accumulation modes and their sources (Lange et



1 al., 2018). Finally, aerosol category *coarse* shows minor occurrence at all three sites (1-  
2 4%).

3

#### 4 **3.2.2 Annual behaviour**

5

6 The *pristine* category did not present a clear annual seasonality at the ZEP and VRS sites,  
7 although at the GRU site it occurred mainly during spring months (Fig. 4a). The *nucleation*  
8 category clearly showed high strong occurrence during summer months at the VRS site.  
9 By contrast, at the Svalbard sites (GRU, ZEP) two main periods dominate in May and in  
10 August (Fig. 4b). Similar trends can be seen for the *bursting* category (Fig. 4c). Whilst at  
11 the VRS site this category shows occurrence similar to the *nucleation* category (Fig. 4b),  
12 the Svalbard sites (GRU, ZEP) mainly occur during spring months. As previously  
13 discussed (Dall'Osto et al., 2017a, Dall'Osto et al., 2018) the lack of gaseous precursors  
14 during spring may be the limiting factors. The two Aitken dominant mode aerosol  
15 categories (*Nascent* and *Nascent broad*) show very similar temporal trends peaking mainly  
16 during summer months at all three stations (Fig. 4d, e). Previous studies already  
17 discussed freshly and locally produced aerosol particles dominating the Arctic summer,  
18 driven by an increase in both biological activity and photochemistry as well as limited long  
19 range transport from mid latitudes (Ström et al., 2009). Therefore, particles are not growing  
20 more than into a pronounced Aitken mode in summer month, particularly in July and  
21 August (Tunved et al., 2013, Dall'Osto et al., 2017a). The two accumulation dominant  
22 aerosol mode categories mainly occur during wintertime. The *accumulation\_150* peaks  
23 mainly during the months of February-April (maximum in March) confirming its association  
24 with the Arctic haze phenomenon (Fig. 4f) in all three stations. By contrast, the larger  
25 *accumulation\_220* mode category occurs during all autumn and winter months, including



1 October-December (Fig. 4g). Finally, the last minor cluster (*coarse*) does not show any  
2 clear trend due to its low frequency (Fig. 4h). The overall annual temporal frequency can  
3 be summarised in Fig. 5, where broader categories can be seen. It is well known that the  
4 Arctic atmosphere is heavily impacted by transport of air pollution from lower latitudes in  
5 spring compared to in summer (Heidam et al., 2004; Law and Stohl, 2007). The continent-  
6 derived winter and spring aerosols, known as Arctic haze, reach their maximum number  
7 concentration during late spring, approximately in April (Tunved et al., 2013; Nguyen et al.  
8 2016) A recent intercomparison of particle number size distributions from several Arctic  
9 stations by Freud et al. (2017) suggests differences between the studied stations  
10 regarding cluster frequency of occurrence throughout the year. The most prominent  
11 differences were observed between the stations at Barrow and Zeppelin, but the GRU site  
12 was not consider in their analysis.

13

14

### 15 **3.2.3 Association of aerosol categories with chemical and physical parameters**

16

17

18 Different chemical species of natural and anthropogenic origin may contribute to the Arctic  
19 aerosol (Tunved et al., 2013; Hirdman et al., 2010). SO<sub>2</sub> in the Arctic has both  
20 anthropogenic and natural sources (Barriel et al., 1986), but in our study it is shown mainly  
21 occurring with large accumulation mode during wintertime (Fig. 6a). Combustion-derived  
22 particles can be transported to the Arctic and can be accompanied by aging of the aerosol  
23 through condensational processes. Our study confirm previous ones where SO<sub>2</sub> was  
24 shown to parallel with black carbon both at VRS and ZEP (Nguyen et al., 2013; Massling  
25 et al., 2015, Dall'Osto et al., 2017a). By contrast, we find the highest concentrations of  
26 ammonia associated with the *nucleation* category. Interestingly, also the two Aitken  
27 dominating mode categories (*nascent* and *nascent broad*) show high concentrations of



1 ammonia (Fig. 6b). Ammonia can impact increasing rates of new particle formation and  
2 growth via stabilization of sulphuric acid clusters (Kirkby et al., 2011). There is growing  
3 interest to better constrain the location, population, and ammonia emissions of the Arctic.  
4 Zooplankton excretion and bacterial remineralization of phytoplankton-derived organic  
5 matter is believed to be a dominant source in the marine environment (Carpenter et al.,  
6 2012) although there remains considerable uncertainty (Lin et al., 2016). The melting of  
7 sea ice is also a significant source of ammonium (Tovar-Sanchez et al., 2010), with  
8 protein-like compounds accumulating in the sea-ice interface (Galgani et al., 2016), similar  
9 processes are also seen in Antarctic sea ice (Dall’Osto et al., 2017b). There is evidence  
10 that coastal seabird colonies are sources of  $\text{NH}_3$  in the summertime Arctic (Wentworth et  
11 al., 2016), although there is still uncertainty (Riddich et al., 2012). Recently, ammonia from  
12 seabirds was found to be a key factor contributing to bursts of newly formed coastal  
13 particles at Alert, Canada (Croft et al., 2016). However, regions of open water and melting  
14 sea ice were found to drive new particle formation in North East Greenland (Dall’Osto et  
15 al., 2018b), such events seem not to be related to bird colonies from coastal zones.

16 The association with selected chemical components measured in aerosols collected at  
17 GRU and ZEP are shown in Fig. 7. It is important to stress that the aerosol chemical  
18 composition shown are derived from  $\text{PM}_{10}$  measurements, and thus does not necessarily  
19 reflect the chemical composition of the aerosol covered by the size distribution analysis  
20 herein presented and discussed. Nevertheless, the comparison may help in apportioning  
21 aerosol sources and processes. Fig 7 (a-c) shows similar trend for three chemical  
22 elements (Cl, Na, Mg). Mechanically generated sea salt particles are normally found in the  
23 coarser size fraction which points to a marine source for Na, Mg and Cl. Indeed, the  
24 highest concentrations are seen for the *coarse* category (about  $350 \text{ ng m}^{-3}$ ,  $300 \text{ ng m}^{-3}$  and  
25  $40 \text{ ng m}^{-3}$  for Cl, Na and Mg, respectively), followed for categories *accumulation\_150*,



1 *accumulation\_220* and *pristine*. Sea spray aerosol (SSA) is generated by bubble bursting  
2 due to surface winds. SSA contributes to the global aerosol burden multiple times more  
3 than the anthropogenic aerosol (Raes et al., 2000; Grythe et al., 2014). Potassium can be  
4 associated with sea salt, although K-rich particles are often also attributed to biomass  
5 burning (Hudson et al., 2004; Moroni et al., 2017), correlating with gas-phase  
6 measurements of acetonitrile, a good biomass-burning tracer. Indeed, accumulation  
7 aerosol categories show high concentrations of potassium (about 25-30 ng m<sup>-3</sup>), but the  
8 trend is not observed for the *pristine* class. Aerosols not only originate from primary  
9 sources like sea spray and biomass burning, but can also be formed via secondary  
10 processes, through chemical transformation of gas-phase species in the atmosphere, most  
11 notably sulphur dioxide, oxides of nitrogen, and volatile organic compounds (Harrison et  
12 al., 1999). Non-sea-salt sulphate (nss-SO<sub>4</sub>) is a mixed source tracer with a large  
13 anthropogenic fossil and biomass fuel component and a smaller biogenic marine  
14 component. Aerosol nitrate is predominantly anthropogenic and arises from the oxidation  
15 of NO<sub>x</sub> from combustion processes associated with vehicles and industrial activity. A  
16 considerable proportion of these acidic nitric and sulphuric aerosols are neutralized in  
17 the atmosphere by NH<sub>3</sub> (Asman et al., 1998). The two categories with the highest  
18 concentrations of sulphate, nitrate and ammonium are found to be *accumulation\_150* and  
19 *accumulation\_220* (about 500 ng m<sup>-3</sup>, 120 ng m<sup>-3</sup> and 65 ng m<sup>-3</sup>, respectively) suggesting  
20 as expected these two are composed of a number of primary and secondary components  
21 of anthropogenic origin. It is interesting to note that ammonium is only partly neutralising  
22 the Arctic aerosols (in average with one-third) and in the Arctic, the aerosols are highly  
23 acidic.

24 Overall, the lowest aerosol mass concentrations seen in Fig. 7 (a-e) are seen for the  
25 *nucleation*, *nascent* and *nascent broad* categories. This is not surprising, because the



1 occurrence of new particle formation events and growth to the Aitken mode is mainly  
2 controlled not only by the precursor gaseous presence but also by pre-existing particle  
3 concentrations (Kulmala et al., 2001). Indeed, these events are often found under low  
4 aerosol concentration conditions in remote areas (Tunved et al., 2013). The low aerosol  
5 mass concentrations associated with these recently formed categories still allow us to  
6 draw some important conclusions about the possible sources forming these new particles  
7 in the Arctic. An opposite trend relative to the previously discussed chemical aerosol  
8 markers can be seen in Fig. 7h showing methane sulphonate (MSA) concentrations  
9 sampled at the GRU monitoring site. The highest concentrations can be seen for the  
10 categories *bursting*, *nucleation*, *nascent* and *nascent broad*. MSA is formed via oxidation  
11 of dimethyl sulfide (DMS), a gas produced by marine phytoplankton (Gali et al., 2015). It is  
12 the most abundant form of biogenic sulphur released from the ocean (Lovelock et al.,  
13 1972; Stefels et al., 2007). Previous studies show that the emission of oceanic DMS may  
14 impact aerosol formation in the Arctic atmosphere (Levasseur et al., 2013; Becagli et al.,  
15 2016, Dall'Osto et al., 2017a). Recent study at the ZEP size shows that during summer,  
16 the impact of the anthropogenic sources upon sulphate is lower (42%), with a contribution  
17 comparable to that coming from biogenic emissions (35%) (Udisti et al., 2016). The  
18 association of MSA not only with the *nucleation* but also with the *bursting* category  
19 suggests that secondary processes may drive both categories, somehow pointing to a  
20 lower ultrafine primary origin association with this particle type. However, it is important to  
21 stress that high uncertainty regarding the mechanism of aerosol production in the Arctic -  
22 especially from leads and open pack ice - still remains (Leck et al., 2002). The interactions  
23 between the surface layer of the ocean and the atmosphere are highly variable and  
24 ecosystem interactions are more important than any single biological variable. For  
25 example, Park et al. (2018) discussed the atmospheric DMS in the Arctic Ocean and its



1 relation to phytoplankton biomass. The DMS production capacity of the Greenland Sea  
2 was estimated to be a factor of three greater than that of the Barents Sea, whereas the  
3 phytoplankton biomass in the Barents Sea was more than two fold greater than that in the  
4 Greenland Sea, stressing the occurrence of a greater abundance of DMS-producing  
5 phytoplankton in the Greenland Sea than in the Barents Sea during the phytoplankton  
6 bloom periods.

7 The chemical nature and origin of the fine particulate matter over Arctic regions, and  
8 especially of its organic fraction, are still largely unknown (Kawamura et al., 1996a, b;  
9 Leaitch et al., 2018). Water-soluble dicarboxylic acids and related polar compounds,  
10 including oxocarboxylic acids and  $\alpha$ -dicarbonyls are ubiquitously found from the ground  
11 surface to the free troposphere (Decesari et al., 2006; Kawamura and Bikkina, 2016).  
12 Primary sources include fossil fuel combustion and burning of biomass and biofuels.  
13 Secondary sources include production via photooxidation of volatile organic compounds  
14 (VOCs) and unsaturated fatty acids (UFAs) derived from anthropogenic and biogenic  
15 sources. VOC sources include wildfire, emissions from snow, ocean, sea ice, boreal forest  
16 and tundra (Tunved et al., 2006; Carpenter et al., 2012, Kos et al., 2014; Haque et al.,  
17 2016, Mungall et al., 2017). For this study, we were able to compare our SMPS aerosol  
18 categorization with two organic chemical species measured at daily time resolution at the  
19 GRU monitoring sites. Results are shown in Figure 8. A clear association can be seen for  
20 oxalic and pyruvic acids, anti-correlating between them. Broadly, in the remote marine  
21 atmosphere, pyruvic acid may be produced by photochemical oxidation of isoprene and  
22 other biogenic volatile organic compounds (BVOCs) emitted from marine biota, which are  
23 finally oxidized to produce oxalic acid (Carlton et al., 2007; Carpenter et al., 2012; Bikkina  
24 et al., 2014). Oxalic acid is often found as the most abundant water-soluble organic  
25 compound, and in-cloud processing is recognized as its major production pathway (Yu et



1 al., 2005). Figure 8 further supports our studies suggesting that the aerosol categories  
2 defined by low mass concentrations and high ultrafine sub-50nm particles are associated  
3 with rather local secondary processes from marine VOC sources. Recent studies have  
4 found that lower organic mass (OM) concentrations but higher ratios of OM to non-sea-salt  
5 sulfate mass concentrations accompany smaller particles during the summer (Leitch et al.,  
6 2018), stressing the importance of marine Arctic organic components responsible for the  
7 ultrafine aerosol population.

8 We conclude this section by reporting the calculated average CCN concentrations  
9 corresponding to each aerosol category. CCN number concentrations influence cloud  
10 microphysical and radiative properties, and consequently the aerosol indirect radiative  
11 forcing (IPCC, 2014). The variability of even low concentrations of CCN is important in the  
12 Arctic, an environment where cloud formation – and hence cloud forcing – is limited by the  
13 CCN availability (Mauritsen et al., 2011). Figure 9 shows that the two accumulation  
14 categories (*accumulation\_150* and *accumulation\_220*) are associated with the highest  
15 CCN concentrations (about 125 particles  $\text{cm}^{-3}$ ) with also the highest ratio of CCN over N.  
16 Usually, ultrafine particles smaller than 100nm in diameter are considered too small to  
17 activate to cloud droplets. However, Leitch et al. (2016) concluded that 20–100 nm  
18 particles from Arctic natural sources can have a broad impact on the range of cloud droplet  
19 number concentrations (CDNC) in clean environments, affirming a large uncertainty in  
20 estimating a baseline for the cloud albedo effect. Changes in pressure and temperature  
21 may not be efficient to generate the required supersaturations needed to activate smaller  
22 particles, with the Kelvin effect acting as limiting factor (Browse et al., 2014; Leitch et al.,  
23 2013). However, the low concentrations of accumulation mode aerosols often found in the  
24 Arctic may lower water vapour uptake rates during droplet formation, and the resulting  
25 increase supersaturation may enable smaller particles to become cloud droplets. The



1 *nascent* and *nascent broad* categories also show associations with high CCN  
2 concentrations despite the much lower average size distributions (Fig. 3d) associated with  
3 these particle types. Despite anthropogenic influence on the accumulation mode is  
4 maintained through winter months, natural sources indeed have a significant impact on  
5 particle number over summer. Hereby these natural sources facilitate aerosol activation to  
6 cloud droplets and thus cloud formation. *Pristine*, *bursting* and *nucleation* categories show  
7 very low associated CCN concentrations (about 50-75 particles  $\text{cm}^{-3}$ ), only about 30% of  
8 the total N being activated. In the previously mentioned study by Dall'Osto et al. (2017a) it  
9 is also shown that the new particle formation (NPF) events and the growth of these aerosol  
10 particles to a larger size can affect the CCN number concentration, reporting an increase  
11 of the CCN number concentration (measured at a supersaturation of 0.4%) of 21%, which  
12 is linked to NPF events. Low level clouds are one of the major players controlling the  
13 radiative balance in the Arctic. Further multidisciplinary studies are needed in order to  
14 understand the processes that determine cloud properties on which particles actually form  
15 cloud droplets under various conditions.

16

17

#### 18 **4 IMPLICATIONS AND CONCLUSIONS**

19

20 Aerosol size distributions sampled simultaneously in three background location in the  
21 Arctic during 2013-2015 (584 days total data coverage simultaneous at 3 stations) were  
22 analyzed by K-means clustering techniques. The K-means analysis identified 8 distinct  
23 aerosol size distributions, representing specific aerosol categories: low particle number  
24 Arctic concentrations (*pristine*, 12-14%), new particle formation and bursts of ultrafine  
25 particles (*nucleation*, 8-21%; *bursting*, 11-21%), ultrafine aerosols dominating the Aitken  
26 mode (*nascent*, 7-21%; *nascent broad*, 10-14%), accumulation dominating aerosol mode



1 (*accumulation\_150*, 13-42%; *accumulation\_220*, 8-19%) and coarse sea spray aerosols  
2 (*coarse*, 1-4%). During winter months, mass concentrations of atmospheric aerosols in the  
3 Arctic are higher compared to summer. Broadly, this is due to differences in the transport  
4 of anthropogenic particles and wet scavenging (Stohl, 2006); local boundary layer height,  
5 stability and stratification also play a role (Brooks et al., 2017). By contrast, total aerosol  
6 number concentrations in the Arctic are often found to be similar throughout the period of  
7 March–September (Tunved et al., 2013). However, the number concentrations in spring  
8 (March–April) are almost exclusively governed by accumulation mode aerosols peaking at  
9 150nm, while the summer concentrations are associated with elevated numbers of Aitken  
10 mode particles and frequent new particle formation events. The main findings of this work  
11 follow:

- 12 • The three monitoring sites experience very pristine low particle number  
13 concentrations only 12-14% of the time.
- 14 • New particle formation and growth and bursts of sub-30nm particles are detected 8-  
15 21% of the time. The lower frequencies detected at the Greenland site (VRS 8%)  
16 relative to the Svalbard sites (ZEP-GRU, 11-21%) are likely due to the former site  
17 being surrounded by the ice stream from the Arctic Ocean and isolated from open  
18 ocean and melting sea ice regions emitting biogenic gas precursors. The Aitken  
19 mode aerosol categories dominate the summer time periods at all sites (19-35%),  
20 but at VRS one has a shorter summer season due to longer sea ice coverage and  
21 14° degrees lower yearly average temperature compared to the stations at  
22 Svalbard.
- 23 • Two types of accumulation mode aerosols are found, one associated with the Arctic  
24 haze peaking in March-April (monomodal at about 150nm) and one seen during the  
25 winter months (monomodal at about 220nm). The site in Greenland (VRS) is



1 exposed to accumulation mode aerosols longer than the one at Svalbard. This is  
2 likely due to different transport pathways into the polar dome, a boundary which  
3 separates cold air in the Arctic from the relatively warm air in midlatitude regions  
4 (Stohl, 2006).

5  
6 The aerosol size distributions data herein compared from three different stations were  
7 intercompared for the first time. The study builds additional knowledge to the findings  
8 presented by Freud et al. (2017), with a focal point on the new particle formation  
9 phenomena as observed in the Arctic environment. This important exercise had to be  
10 carried out, and the expected results - although not striking - set the ground for important  
11 future studies. In the future, a decrease in sea ice coverage across the Arctic Ocean may  
12 increase the annual primary production (Arrigo et al., 2008), and may alter species  
13 composition of phytoplankton (Fujiwara et al., 2014). Hence, the emissions of biogenic  
14 sulphur gases that are aerosol precursors and hence affect aerosol growth and formation  
15 would increase change in summer. In this regard, the location of the monitoring sites at  
16 Svalbard and Greenland are ideal to study aerosol formation and transport across the two  
17 different regions. The two stations are separated by the Greenland Sea, a highly  
18 productive region with a great abundance of DMS-producing phytoplankton (Park et al.,  
19 2018). As the DMS production capacity of the ocean depends critically on the  
20 phytoplankton species composition and the complex food web mechanisms (Stefels et al.,  
21 2007), multidisciplinary studies across these regions are warranted. The recent  
22 transformations in the Arctic and their global causes and consequences have put  
23 international cooperation in the Arctic Council at the forefront of research in governance  
24 (Knecht et al., 2016). Larger atmospheric chemistry and physics datasets are being  
25 collected by a number of countries, and this work highlights the benefit that can be gained



1 from international cooperation. Given that the present work has validated the quality of the  
2 presented aerosol size distributions, these data will be used again to address specific  
3 questions, including vertical transport (i.e. the two sites at the Svalbard) and horizontal  
4 transport (i.e. Arctic aerosol transport from Greenland to Svalbard regions). The significant  
5 costs associated with these types of coordinated international collaborations can provide  
6 far more information than individual sites operating on their own. This may help to  
7 understand better the complex interactions and feedbacks between the aerosol, the  
8 clouds, the longwave and shortwave radiation, the ocean dynamics, the biota and the  
9 environment (Browse et al., 2014). Special concern is arising also from increasing  
10 navigability in the rapidly melting Arctic Ocean with expanding community re-supply,  
11 fishing, tourism, fossil fuel exploitation and cargo trading, which is projected to cause a  
12 large increase in emissions by 2050 (Melia et al., 2016). Future studies looking  
13 simultaneously at different Arctic monitoring sites will reduce the uncertainties in future  
14 projections of Arctic climate changes and its implications for our planet (Koivurova et al.,  
15 2012; Byers, 2013; Conde Perez et al., 2016). Our study supports international  
16 environmental cooperation concerning the Arctic region.

17

## 18 REFERENCES

19 Arrigo, K. R., van Dijken, G., & Pabi, S. Impact of a shrinking Arctic ice cover on marine  
20 primary production. *Geophysical Research Letters*, 35, L19603.  
21 <https://doi.org/10.1029/2008GL035028>, 2008

22

23 Asmi, E., Kondratyev, V., Brus, D., Laurila, T., Lihavainen, H., Backman, J., Vakkari, V.,  
24 Aurela, M., Hatakka, J., Viisanen, Y., Uttal, T., Ivakhov, V., and Makshtas, A.: Aerosol size  
25 distribution seasonal characteristics measured in Tiksi, Russian Arctic, *Atmos. Chem.*  
26 *Phys.*, 16, 1271-1287, <https://doi.org/10.5194/acp-16-1271-2016>, 2016.

27

28 Barriol, A. Arctic air pollution: An overview of current knowledge. *Atmos. Environ.* 20, 643–  
29 663, 1986



1

2 Becagli, S., Lazzara, L., Marchese, C., Dayan, U., Ascanius, S. E., Cacciani, M., Caiazza,  
3 L., Di Biagio, C., Di Iorio, T., di Sarra, A., Eriksen, P., Fani, F., Giardi, F., Meloni, D.,  
4 Muscari, G., Pace, G., Severi, M., Traversi, R., and Udisti, R.: Relationships linking  
5 primary production, sea ice melting, and biogenic aerosol in the Arctic, *Atmos. Environ.*,  
6 136, 1–15, <https://doi.org/10.1016/j.atmosenv.2016.04.002>, 2016.

7

8 Beddows, D. C. S., Dall'Osto, M., and Harrison, R. M.: Cluster Analysis of Rural, Urban  
9 and Curbside Atmospheric Particle Size Data, *Environ. Sci. Technol.*, 43, 4694–4700,  
10 2009.

11

12 Beddows, D. C. S., Dall'Osto, M., Harrison, R. M., Kulmala, M., Asmi, A., Wiedensohler,  
13 A., Laj, P., Fjaeraa, A. M., Sellegri, K., Birmili, W., Bukowiecki, N., Weingartner, E.,  
14 Baltensperger, U., Zdimal, V., Zikova, N., Putaud, J.-P., Marinoni, A., Tunved, P.,  
15 Hansson, H.-C., Fiebig, M., Kivekäs, N., Swietlicki, E., Lihavainen, H., Asmi, E., Ulevicius,  
16 V., Aalto, P. P., Mihalopoulos, N., Kalivitis, N., Kalapov, I., Kiss, G., de Leeuw, G.,  
17 Henzing, B., O'Dowd, C., Jennings, S. G., Flentje, H., Meinhardt, F., Ries, L., Denier van  
18 der Gon, H. A. C., and Visschedijk, A. J. H.: Variations in tropospheric submicron particle  
19 size distributions across the European continent 2008–2009, *Atmos. Chem. Phys.*, 14,  
20 4327–4348, <https://doi.org/10.5194/acp-14-4327-2014>, 2014.

21

22 Bikkina, S., K. Kawamura, Y. Miyazaki, and P. Fu High abundance of oxalic, azelaic, and  
23 glyoxylic acids and methylglyoxal in the open ocean with high biological activity:  
24 Implication for secondary SOA formation from isoprene, *Geophys. Res. Lett.*, 41, 3649–  
25 3657, doi:10.1002/2014GL059913, 2014

26

27 Brooks, I.M., Tjernström, M., Persson, P.O.G., Shupe, M.D., Atkinson, R.A., Canut, G.,  
28 Birch, C.E., Mauritsen, T., Sedlar, J., Brooks, B.J. The turbulent structure of the Arctic  
29 summer boundary layer during the Arctic summer cloud-ocean study. *J. Geophys. Res.:*  
30 *Atmosphere* 122, 9685–9704. <http://dx.doi.org/10.1002/2017JD027234>, 2017

31

32 Browse, J., Carslaw, K. S., Mann, G.W., Birch, C. E., Arnold, S. R., and Leck, C.: The  
33 complex response of Arctic aerosol to sea-ice retreat, *Atmos. Chem. Phys.*, 14, 7543–  
34 7557, doi:10.5194/acp-14-7543-2014, 2014.

35

36 Byers, M., *International Law and the Arctic*. Cambridge University Press,  
37 Cambridge., 2013

38

39 Carlton, A. G., B. J. Turpin, K. E. Altieri, S. Seitzinger, A. Reff, H.-J. Lim, and B. Ervens  
40 Atmospheric oxalic acid and SOA production from glyoxal: Results of aqueous  
41 photooxidation experiments, *Atmos. Environ.*, 41, 7588–7602, 2007

42



- 1 Carlton, A. G., Wiedinmyer, C., and Kroll, J. H.: A review of Secondary Organic Aerosol  
2 (SOA) formation from isoprene, Atmos. Chem. Phys., 9, 4987-5005,  
3 <https://doi.org/10.5194/acp-9-4987-2009>, 2009.
- 4
- 5 Carslaw, K. S., Lee, L. A., Reddington, C. L., Pringle, K. J., Rap, A., Forster, P. M., Mann,  
6 G. W., Spracklen, D. V., Woodhouse, M. T., Regayre, L. A., and Pierce, J. R.: Large  
7 contribution of natural aerosols to uncertainty in indirect forcing, Nature, 503, 67–71,  
8 doi:10.1038/nature12674, 2013.
- 9
- 10 Carpenter, L. J., Archer, S. D. & Beale, R. Ocean-atmosphere trace gas exchange. Chem.  
11 Soc. Rev. 41, 6473–6506, doi:10.1039/c2cs35121h, 2012
- 12
- 13 Cohen J, Screen JA, Furtado JC, Barlow M, Whittleston D, Coumou D, Francis J, Dethloff  
14 K, Entekhabi D, Overland J, et al. Recent Arctic amplification and extreme mid - latitude  
15 weather. Nat Geosci , 7:627–637., 2014
- 16
- 17 Conde Perez, E., Valerieva Yaneva, Z.. The European Arctic policy in progress. Polar Sci.  
18 10 (3), 441e449, 2016
- 19
- 20 Croft, B., Wentworth, G. R., Martin, R. V., Leaitch, W. R., Murphy, J. G., Murphy, B. N.,  
21 Kodros, J., Abbatt, J. P. D., and Pierce, J. R.: Contribution of Arctic seabird-colony  
22 ammonia to atmospheric particles and cloud-albedo radiative effect, Nat. Commun., 7,  
23 13444, doi:10.1038/ncomms13444, 2016
- 24
- 25 Dall'Osto, M., Monahan, C., Greaney, R., Beddows, D. C. S., Harrison, R. M., Ceburnis,  
26 D., and O'Dowd, C. D.: A statistical analysis of North East Atlantic (submicron) aerosol  
27 size distributions, Atmos. Chem. Phys., 11, 12567-12578, doi:10.5194/acp-11-12567-  
28 2011, 2011
- 29
- 30 Dall'Osto, M., Beddows, D. C. S., Tunved, P., Krejci, R., Ström, J., Hansson, H.-C., Yoon,  
31 Y. J., Park, K.-T., Becagli, S., Udisti, R., Onasch, T., O'Dowd, C. D., Simó, R., and  
32 Harrison, R. M.: Arctic sea ice melt leads to atmospheric new particle formation, Sci. Rep.,  
33 7, 3318, <https://doi.org/10.1038/s41598-017-03328-1>, 2017a.
- 34
- 35 Dall'Osto, M., Ovadnevaite, J., Paglione, M., Beddows, D. C., Ceburnis, D., Cree, C.,  
36 Cortés, P., Zamanillo, M., Nunes, S. O., Pérez, G. L., Ortega-Retuerta, E., Emelianov, M.,  
37 Vaqué, D., Marrasé, C., Estrada, M., Sala, M. M., Vidal, M., Fitzsimons, M. F., Beale, R.,  
38 Airs, R., Rinaldi, M., Decesari, S., Facchini, M. C., Harrison, R. M., O'Dowd, C., and Simó,  
39 R.: Antarctic sea ice region as a source of biogenic organic nitrogen in aerosols, Sci. Rep.,  
40 7, 6047, <https://doi.org/10.1038/s41598-017-06188-x>, 2017b.
- 41



- 1 Dall'Osto, M., D.C.S. Beddows, A. Asmi, L. Poulain, L. Hao, E. Freney, J.D. Allan, M.  
2 Canagaratna, M. Crippa, F. Bianchi, G. de Leeuw, A. Eriksson, E. Swietlicki, H.C.  
3 Hansson, J.S. Henzing, C. Granier, K. Zemann, P. Laj, T. Onasch, A. Prevot, J.P.  
4 Putaud, K. Sellegri, M. Vidal, A. Virtanen, R. Simo, D. Worsnop, C. O'Dowd, M. Kulmala,  
5 R.M. Harrison, Novel insights on new particle formation derived from a paneuropean  
6 observing system, *Sci. Rep.* 8 (2018)1482, 2018a  
7  
8 Dall'Osto, M., Lange, R., Geels, C., Beddows, D.C.S., Harrison, R.M., Simo, R.,  
9 Boertmann, D., Skov, H., Massling, A., 2018. Open pack ice drives new particle formation  
10 in North East Greenland. *Sci. Rep. (In press)*., 2018b  
11  
12 Decesari, S., Fuzzi, S., Facchini, M.C., Mircea, M., Emblico, L., Cavalli, F., Maenhaut,  
13 W., Chi, X., Schkolnik, G., Falkovich, A., Rudich, Y., Claeys, M., Pashynska, V., Vas, G.,  
14 Kourtchev, I., Vermeylen, R., Hoffer, A., Andreae, M.O., Tagliavini, E., Moretti, F., Artaxo,  
15 P. Characterization of the organic composition of aerosols from Rondonia, Brazil, during  
16 the LBA-SMOCC 2002 experiment and its representation through model compounds.  
17 *Atmos. Chem. Phys.* 6, 375–402, 2006  
18  
19 Freud, E., Krejci, R., Tunved, P., Leaitch, R., Nguyen, Q. T., Massling, A., Skov, H., and  
20 Barrie, L.: Pan-Arctic aerosol number size distributions: seasonality and transport patterns,  
21 *Atmos. Chem. Phys.*, 17, 8101-8128, <https://doi.org/10.5194/acp-17-8101-2017>, 2017.  
22  
23 Fujiwara, A., Hirawake, T., Suzuki, K., Imai, I., and Saitoh, S.-I.: Timing of sea ice retreat  
24 can alter phytoplankton community structure in the western Arctic Ocean, *Biogeosciences*,  
25 11, 1705-1716, <https://doi.org/10.5194/bg-11-1705-2014>, 2014.  
26  
27 Galgani, L., Piontek, J., Engel, A.. Biopolymers form a gelatinous microlayer at the air-sea  
28 interface when Arctic sea ice melts. *Sci. Rep.* 6, 29465. [http://](http://dx.doi.org/10.1038/srep29465)  
29 [dx.doi.org/10.1038/srep29465](http://dx.doi.org/10.1038/srep29465), 2016  
30  
31 Galí, M., Devred, E., Levasseur, M., Royer, S., & Babin, M. A remote sensing algorithm for  
32 planktonic dimethylsulfoniopropionate (DMSP) and an analysis of global patterns. *Remote*  
33 *Sensing of Environment*, 171, 171–184. <https://doi.org/10.1016/j.rse.2015.10.012>, 2015  
34  
35 Grythe, H., Ström, J., Krejci, R., Quinn, P., and Stohl, A.: A review of sea-spray aerosol  
36 source functions using a large global set of sea salt aerosol concentration measurements,  
37 *Atmos. Chem. Phys.*, 14, 1277–1297, doi:10.5194/acp-14-1277-2014, 2014.  
38  
39 Harrison, R. M., et al. (Eds.), *Source Apportionment of Airborne Particulate Matter in the*  
40 *United Kingdom: The First Report of the Airborne Particles Expert Group*, Dep. of the  
41 *Environ., Transp. and Reg.*, London, 1999  
42



- 1 Haque, M.M., Kawamura, K., Kim, Y. Seasonal variations of biogenic secondary organic  
2 aerosol tracers in ambient aerosols from Alaska. *Atmos. Environ.* 130, 95–104, 2016.  
3  
4 Heidam, N.Z., Christensen, J., Wahlin, P., Skov, H. Arctic atmospheric contaminants in NE  
5 Greenland: levels, variations, origins, transport, transformations and trends 1990-2001.  
6 *Sci. Total Environ.* 331 (1–3), 5–28. <http://dx.doi.org/10.1016/j.scitotenv.2004.03.033>,  
7 2004  
8  
9 Hirdman, D. et al. Source identification of short-lived air pollutants in the Arctic using  
10 statistical analysis of measurement data and particle dispersion model output. *Atmos*  
11 *Chem Phys* 10, 669–693, 2010  
12  
13 Hogrefe O, Lala GG, Frank BP, Schwab JJ, Demerjian KL Field evaluation of a TSI 3034  
14 scanning mobility particle sizer in New York City: Winter 2004 intensive campaign. *Aerosol*  
15 *Sci Technol* 40:753–762, 2006  
16  
17 Hudson, P.K., Murphy, D.M., Cziczo, D.J., Thomson, D.S., de Gouw, J.A., Warneke, C.,  
18 Holloway, J., Jost, J.R., Hubler, G. Biomass-burning particle measurements: Characteristic  
19 composition and chemical processing. *Journal of Geophysical Research—Atmospheres*  
20 109 (D23) (Article no. D23S27), 2004  
21  
22 IPCC, 2014. *Climate Change 2014: Impacts, Adaptation, and Vulnerability*, 2014  
23  
24 Kawamura, K., Bikina, S.. A review of dicarboxylic acids and related compounds in  
25 atmospheric aerosols: molecular distributions, sources and transformation. *Atmos. Res.*  
26 170, 140–160., 2016  
27  
28 Kawamura, K., H. Kasukabe, and L. A. Barrie, Source and reaction pathways of  
29 dicarboxylic acids, ketoacids and dicarbonyls in arctic aerosols: One year of observations,  
30 *Atmos. Environ.*, 30, 1709–1722, 1996a  
31  
32 Kawamura, K., R. Sempéré, Y. Imai, M. Hayashi, and Y. Fujii, Water soluble dicarboxylic  
33 acids and related compounds in the arctic aerosols, *J. Geophys. Res.*, 101, 18,721–  
34 18,728, doi:10.1029/96JD01541, 1996b  
35  
36 Kirkby, J., Curtius, J., Almeida, J., Dunne, E., Duplissy, J., Ehrhart, S., Franchin, A.,  
37 Gagné, S., Ickes, L., Kürten, A., Kupc, A., Metzger, A., Riccobono, F., Rondo, L.,  
38 Schobesberger, S., Tsagkogeorgas, G., Wimmer, D., Amorim, A., Bianchi, F.,  
39 Breitenlechner, M., David, A., Dommen, J., Downard, A., Ehn, M., Flagan, R. C., Haider, S.,  
40 Hansel, A., Hauser, D., Jud, W., Junninen, H., Kreissl, F., Kvashin, A., Laaksonen, A.,  
41 Lehtipalo, K., Lima, J., Lovejoy, E. R., Makhmutov, V., Mathot, S., Mikkilä, J., Minginette, P.,  
42 Mogo, S., Nieminen, T., Onnela, A., Pereira, P., Petäjä, T., Schnitzhofer, R., Seinfeld, J. H.,



- 1 Sipilä, M., Stozhkov, Y., Stratmann, F., Tomé, A., Vanhanen, J., Viisanen, Y., Vrtala, A.,  
2 Wagner, P. E., Walther, H., Weingartner, E., Wex, H., Winkler, P. M., Carslaw, K. S.,  
3 Worsnop, D. R., Baltensperger, U., and Kulmala, M.: Role of sulphuric acid, ammonia and  
4 galactic cosmic rays in atmospheric aerosol nucleation, *Nature*, 476, 429–33,  
5 <https://doi.org/10.1038/nature10343>, 2011.
- 6
- 7 Knecht, S. “The Politics of Arctic International Cooperation: Introducing a Dataset on  
8 Stakeholder Participation in Arctic Council Meetings, 1998–2015.” *Cooperation and  
9 Conflict*, 2016.
- 10
- 11 Koivurova, T., et al., The present and the future competence of the European Union in the  
12 Arctic. *Polar Rec.* 48 (4), 361e371, 2012
- 13
- 14 Kos, G., V. Kanthasami, N. Adechina, and P. A. Ariya. Volatile organic compounds in  
15 Arctic snow: Concentrations and implications for atmospheric processes, *Environ. Sci.  
16 Process. Impact.*, 16(11), 2592–2603, doi:10.1039/c4em00410h, 2014
- 17
- 18 Kulmala, M., Dal Maso, M., Mäkelä, J. M., Pirjola, L., Väkevä, M., Aalto, P., Mikkulainen,  
19 P., Hämeri, K., and O’Dowd, C. D.: On the formation, growth and composition of nucleation  
20 mode particles, *Tellus B*, 53, 479–490, 2001.
- 21
- 22 Lange et al., Characterization of distinct Arctic aerosol accumulation modes and their  
23 sources. *Atmospheric Environment* 183 (2018) 1–10, 2018
- 24
- 25 Latham, T.L., Beyersdorf, A.J., Thornhill, K.L., Winstead, E.L., Cubison, M.J., Hecobian, A.,  
26 Jimenez, J.L., Weber, R.J., Anderson, B.E., Nenes, A., 2013. Analysis of CCN activity of  
27 Arctic aerosol and Canadian biomass burning during summer 2008. *Atmos. Chem. Phys.*  
28 13 (5), 2735–2756. <http://dx.doi.org/10.5194/acp-13-2735-2013>.
- 29
- 30 Leck, C., Norman, M., Bigg, E. K., and Hillamo, R.: Chemical composition and sources of  
31 the high Arctic aerosol relevant for cloud formation, *J. Geophys. Res.*, 107, 4135,  
32 <https://doi.org/10.1029/2001JD001463>, 2002.
- 33
- 34 Leaitch, W. R., Sharma, S., Huang, L., Toom-Sauntry, D., Chivulescu, A., Macdonald, A.  
35 M., von Salzen, K., Pierce, J. R., Bertram, A. K., Schroder, J. C., Shantz, N. C., Chang, R.  
36 Y.-W., and Norman, A.-L.: Dimethyl sulfide control of the clean summertime Arctic aerosol  
37 and cloud, *Elem. Sci. Anthr.*, 1, 000017, <https://doi.org/10.12952/journal.elementa.000017>,  
38 2013.
- 39
- 40 Leaitch, W. R., Russell, L. M., Liu, J., Kolonjari, F., Toom, D., Huang, L., Sharma, S.,  
41 Chivulescu, A., Veber, D., and Zhang, W.: Organic functional groups in the submicron



- 1 aerosol at 82.5°N, 62.5°W from 2012 to 2014, Atmos. Chem. Phys., 18, 3269-3287,  
2 <https://doi.org/10.5194/acp-18-3269-2018>, 2018.  
3
- 4 Levasseur, M. Impact of Arctic meltdown on the microbial cycling of sulphur. Nat Geosci 6,  
5 691-700, doi:10.1038/Ngeo1910, 2013.  
6
- 7 Lin, C. T. et al. Aerosol isotopic ammonium signatures over the remote Atlantic Ocean.  
8 Atmos. Environ. 133, 165–169, 2016  
9
- 10 Law, K.S., Stohl, A.. Arctic air pollution: origins and impacts. Science 315 (5818),1537–  
11 1540. <http://dx.doi.org/10.1126/science.1137695>, 2007  
12
- 13 Leaitch, W. R., Korolev, A., Aliabadi, A. A., Burkart, J., Willis, M. D., Abbatt, J. P. D.,  
14 Bozem, H., Hoor, P., Köllner, F., Schneider, J., Herber, A., Konrad, C., and Brauner, R.:  
15 Effects of 20–100 nm particles on liquid clouds in the clean summertime Arctic, Atmos.  
16 Chem. Phys., 16, 11107-11124, <https://doi.org/10.5194/acp-16-11107-2016>, 2016.  
17
- 18 Lovelock, J. E., Maggs, R. J., & Rasmussen, R. A.. Atmospheric dimethyl sulphide and the  
19 natural sulphur cycle. Nature, 237(5356),452–453. <https://doi.org/10.1038/237452a0>, 1972  
20
- 21 Massling, A., Nielsen, I. E., Kristensen, D., Christensen, J. H., Sørensen, L. L., Jensen, B.,  
22 Nguyen, Q. T., Nøjgaard, J. K., Glasius, M., and Skov, H.: Atmospheric black carbon and  
23 sulfate concentrations in Northeast Greenland, Atmos. Chem. Phys., 15, 9681-9692,  
24 <https://doi.org/10.5194/acp-15-9681-2015>, 2015.  
25
- 26 Mauritsen, T., Sedlar, J., Tjernström, M., Leck, C., Martin, M., Shupe, M., Sjogren, S.,  
27 Sierau, B., Persson, P. O. G., Brooks, I. M., and Swietlicki, E.: An Arctic CCN-limited  
28 cloud-aerosol regime, Atmos. Chem. Phys., 11, 165-173, <https://doi.org/10.5194/acp-11-165-2011>, 2011.  
29  
30
- 31 Melia, N., K. Haines, and E. Hawkins. Sea ice decline and 21st century trans-Arctic  
32 shipping routes, Geophys. Res. Lett., 43, 9720–9728, doi:10.1002/2016GL069315, 2016  
33
- 34 Moroni B., D. Cappelletti, S. Crocchianti, S. Becagli, L. Caiazza, R. Traversi, R. Udisti, M.  
35 Mazzola, K. Markowicz, C. Ritter, T. Zielinski. Morphochemical characteristics and mixing  
36 state of long range transported wildfire particles at Ny-Ålesund (Svalbard Islands). Atmos.  
37 Environ., 156, 135-145, <http://dx.doi.org/10.1016/j.atmosenv.2017.02.037>. 2017.  
38
- 39 Mungall, E. L., Abbatt, J. P. D., Wentzell, J. J. B., Lee, A. K. Y., Thomas, J. L., Blais, M.,  
40 Gosselin, M., Miller, L. A., Papakyriakou, T., Willis, M. D., and Liggio, J.: A novel source of



- 1 oxygenated volatile organic compounds in the summertime marine Arctic boundary layer,  
2 P. Natl. Acad. Sci. USA, 114, 6203–6208, <https://doi.org/10.1073/pnas.1620571114>, 2017.  
3
- 4 Nguyen, Q. T., Skov, H., Sørensen, L. L., Jensen, B. J., Grube, A. G., Massling, A.,  
5 Glasius, M., and Nøjgaard, J. K.: Source apportionment of particles at Station Nord, North  
6 East Greenland during 2008–2010 using COPREM and PMF analysis, Atmos. Chem.  
7 Phys., 13, 35–49, <https://doi.org/10.5194/acp-13-35-2013>, 2013.  
8
- 9 Nguyen, Q. T., Glasius, M., Sørensen, L. L., Jensen, B., Skov, H., Birmili, W.,  
10 Wiedensohler, A., Kristensson, A., Nøjgaard, J. K., and Massling, A.: Seasonal variation of  
11 atmospheric particle number concentrations, new particle formation and atmospheric  
12 oxidation capacity at the high Arctic site Villum Research Station, Station Nord, Atmos.  
13 Chem. Phys., 16, 11319–11336, <https://doi.org/10.5194/acp-16-11319-2016>, 2016.  
14
- 15 Nordli, Ø., R. Przybylak, A. Ogilvie, and K. Isaksen, Long-term temperature trends and  
16 variability on Spitsbergen: The extended Svalbard Airport temperature series, 1898–2012,  
17 Polar Res., 33, doi:10.3402/polar.v33.21349, 2014  
18
- 19 O'Dowd, C. D. et al. Marine aerosol formation from biogenic iodine emissions. Nature 417,  
20 632–636, doi:10.1038/nature00775, 2002  
21
- 22 Park, K.-T., Lee, K., Kim, T.-W., Yoon, Y. J., Jang, E.-H., Jang, S., et al. Atmospheric DMS  
23 in the Arctic Ocean and its relation to phytoplankton biomass. Global Biogeochemical  
24 Cycles, 32. <https://doi.org/10.1002/2017GB005805>, 2018  
25
- 26 Pithan, F. and Mauritsen, T.: Arctic amplification dominated by temperature feedbacks in  
27 contemporary climate models, Nat. Geosci., 7, 181–184, doi:10.1038/ngeo2071, 2014.  
28
- 29 Raes, F., R. Van Dingenen, E. Vignati, J. Wilson, J. P. Putaud, J. H. Seinfeld, and P.  
30 Adams, Formation and cycling of aerosols in the global troposphere, Atmos. Environ.,  
31 34(25), 4215–4240, 2000  
32
- 33 Riddick, S. N. et al. The global distribution of ammonia emissions from seabird colonies.  
34 Atmos. Environ. 55, 319–327, 2012  
35
- 36 Sipilä, M. et al. Molecular-scale evidence of aerosol particle formation via sequential  
37 addition of HIO<sub>3</sub>. Nature 1-3, <https://doi.org/10.1038/nature19314> (2016)  
38
- 39 Stefels, J., Steinke, M., Turner, S., Malin, G., & Belviso, S. Environmental constraints on  
40 the production and removal of the climatically active gas dimethylsulphide (DMS) and



- 1 implications for ecosystem modeling. *Biogeochemistry*, 83(1-3), 245–275.  
2 <https://doi.org/10.1007/s10533-007-9091-5>, 2007  
3
- 4 Stohl, A. Characteristics of atmospheric transport into the Arctic troposphere. *J. Geophys.*  
5 *Res. Atmos.* 111 (D11). <http://dx.doi.org/10.1029/2005jd006888>, 2006  
6
- 7 Strom, J., Umegard, J., Torseth, K., Tunved, P., Hansson, H. C., Holmen, K., Wisman, V.,  
8 Herber, A., and Konig-Langlo, G.: One year of particle size distribution and aerosol  
9 chemical composition measurements at the Zeppelin Station, Svalbard, March 2000–March  
10 2001, *Phys. Chem. Earth*, 28, 1181–1190, doi:10.1016/j.pce.2003.08.058, 2003.  
11
- 12 Ström, J., Engvall, A.-C., Delbart, F., Krejci, R., and Treffeisen, R.: On small particles in the  
13 Arctic summer boundary layer: observations at two different heights near Ny-Ålesund,  
14 Svalbard, *Tellus B*, 61, 473–482, <https://doi.org/10.1111/j.1600-0889.2008.00412.x>, 2009.  
15
- 16 Tovar - Sánchez, A., C. M. Duarte, J. C. Alonso, S. Lacorte, R. Tauler, and C.  
17 Galbán - Malagón. Impacts of metals and nutrients released from melting multiyear Arctic  
18 sea ice, *J. Geophys. Res.*, 115, C07003, doi:10.1029/2009JC005685, 2010  
19
- 20 Tunved, P., Hansson, H.-C., Kulmala, M., Aalto, P., Viisanen, Y., Karlsson, H.,  
21 Kristensson, A., Swietlicki, E., Dal Maso, M., Ström, J., and Komppula, M.: One year  
22 boundary layer aerosol size distribution data from five nordic background stations, *Atmos.*  
23 *Chem. Phys.*, 3, 2183–2205, <https://doi.org/10.5194/acp-3-2183-2003>, 2003.  
24
- 25 Tunved, P., Hansson, H.C., Kerminen, V.M., Strom, J., Dal Maso, M., Lihavainen, H.,  
26 Viisanen, Y., Aalto, P.P., Komppula, M., Kulmala, M. High natural aerosol loading over  
27 boreal forests. *Science* 312, 261–263, 2006  
28
- 29 Tunved, P., Ström, J., and Krejci, R.: Arctic aerosol life cycle: linking aerosol size  
30 distributions observed between 2000 and 2010 with air mass transport and precipitation at  
31 Zeppelin station, Ny-Ålesund, Svalbard, *Atmos. Chem. Phys.*, 13, 3643–3660,  
32 <https://doi.org/10.5194/acp-13-3643-2013>, 2013.  
33
- 34 Udisti R, Bazzano A, Becagli S, Bolzacchini E, et al. Sulfate source apportionment in the  
35 Ny Å lesund (Svalbard Islands) Arctic aerosol. *Rend Fis Acc Lincei*. doi:10.1007/s12210-  
36 016- 0517-7, 2016  
37
- 38 Yu, J. Z., Huang, X.-F., Xu, J., and Hu, M.: When aerosol sulfate goes up, so does oxalate:  
39 implication for the formation mechanisms of oxalate, *Environ. Sci. Technol.*, 29, 128–133,  
40 2005  
41



1 Weber, R. J. et al. A study of new particle formation and growth involving biogenic and  
2 trace gas species measured during ACE 1. *J Geophys Res-Atmos* 103, 16385-16396,  
3 doi:10.1029/97jd02465, 1998

4

5 Wentworth, G. R. et al. Ammonia in the summertime Arctic marine boundary layer:  
6 sources, sinks, and implications. *Atmos. Chem. Phys.* 16, 1937–1953, doi:10.5194/acp-16-  
7 1937-2016, 2016

8

9

## 10 **Acknowledgements**

11 The study was supported by the Spanish Ministry of Economy through project BIO-NUC  
12 (CGL2013-49020-R), PI-ICE (CTM2017-89117-R) and the Ramon y Cajal fellowship  
13 (RYC-2012-11922). The research leading to these results has received funding from the  
14 European Union's Horizon 2020 research and innovation programme under grant  
15 agreement No 654109 and previously from the European Union Seventh Framework  
16 Programme (FP7/2007-2013) under grant agreement n° 262254. The authors would like to  
17 acknowledge the Swedish EPA (Naturvårdsverket) and the Swedish Research Council  
18 Formas for the financial support. The work at Villum Research Station, Station Nord, was  
19 financially supported by the Danish Environmental Protection Agency via the  
20 MIKA/DANCEA funds for Environmental Support to the Arctic Region, which is part of the  
21 Danish contribution to the Arctic Monitoring and Assessment Programme (AMAP) and to  
22 the Danish research project "Short-Lived Climate Forcers" (SLCF). The Villum Foundation  
23 is acknowledged for funding the construction of Villum Research Station, Station Nord.  
24 CCN measurements are supported by a KOPRI program (PN18081), funded by National  
25 Research Foundation of Korea Grant (NRF-2016M1A5A1901769). Data used in this article  
26 are archived and accessible from the EBAS database operated at the Norwegian Institute  
27 for Air Research (NILU) (<http://ebas.nilu.no>). Data management is provided by the WMO  
28 Global Atmosphere Watch World Data Centre for Aerosol. This project has received  
29 funding from the European Union's Horizon 2020 research and innovation programme  
30 under grant agreement No 654109 (ACTRIS).

31

## 32 **Author information**



1 The authors declare no competing financial interests. Correspondence and requests for  
2 materials should be addressed to M.D. ([dallosto@icm.csic.es](mailto:dallosto@icm.csic.es)).

3  
4  
5  
6  
7  
8  
9  
10  
11  
12  
13  
14  
15  
16  
17  
18  
19  
20  
21  
22  
23  
24  
25  
26  
27  
28  
29  
30  
31  
32  
33  
34  
35  
36  
37  
38  
39  
40  
41  
42  
43  
44  
45  
46  
47  
48

1  
2  
3  
4  
5  
6  
7**LIST OF TABLES**

<b>Aerosol category</b>	<b>GRU</b>	<b>ZEP</b>	<b>VRS</b>
(1) <i>Pristine</i>	13	12	14
(2) <i>Nucleation</i>	11	15	8
(3) <i>Bursting</i>	21	14	8
(4) <i>Nascent</i>	21	11	7
(5) <i>Nascent Broad</i>	14	10	11
(6) <i>Accumulation 150</i>	13	14	42
(7) <i>Accumulation 220</i>	6	19	8
(8) <i>Coarse</i>	2	4	1
<b>Total</b>	<b>100</b>	<b>100</b>	<b>100</b>

<i>Summary of main aerosol modes</i>			
<i>Pristine (1)</i>	13	12	14
<i>Nucleation (2,3)</i>	32	29	16
<i>Aitken (4,5)</i>	35	21	19
<i>Accumulation (6,7,8)</i>	20	38	52
<i>Total</i>	100	100	100

8  
9  
10  
11  
12  
13  
14  
15  
16  
17  
18  
19  
20  
21  
22  
23  
24  
25  
26  
27  
28  
29  
30  
31  
32

**Table 1. Occurrence of the K-means cluster analysis featuring the eight aerosol categories detected at the three monitoring sites. At the bottom of the table reported are general aerosol size distribution modes representing as sum of selected aerosol categories.**



1  
2  
3  
4  
5  
6  
7  
8  
9  
10  
11  
12  
13  
14  
15  
16  
17  
18  
19  
20  
21

## LIST OF FIGURES

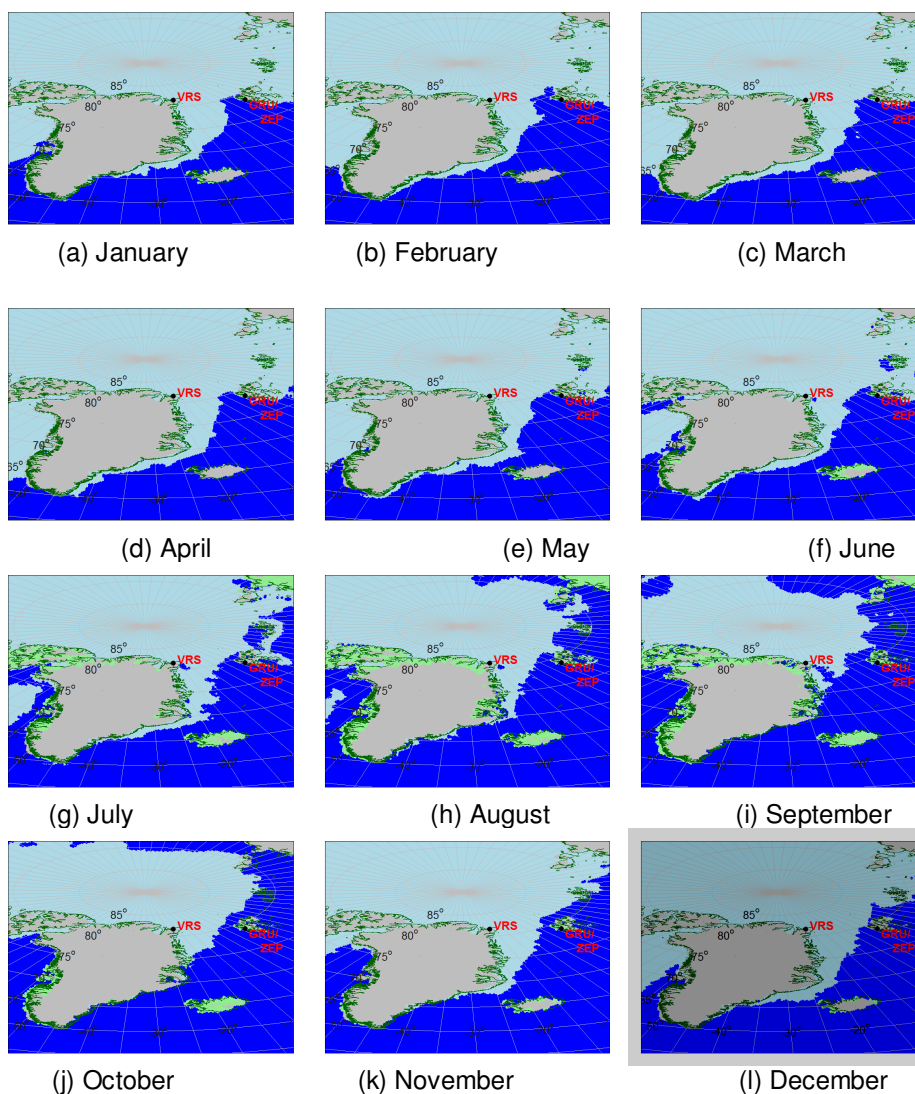
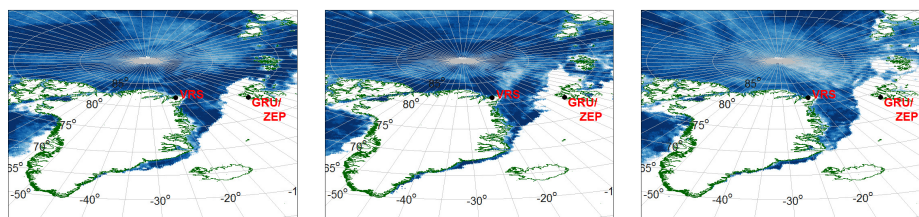


**Figure 1a.** Sea ice (light blue), open water (dark blue), snow on land (grey) and land (light green) maps for the period March-October (a-h). Land borders are marked in dark green.



1  
2

3  
4  
5

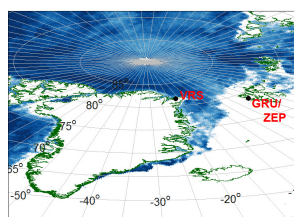


6  
7

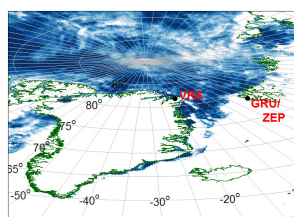
(a) January

(b) February

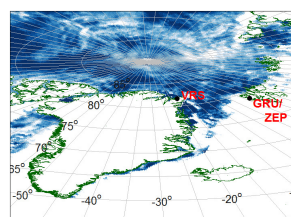
(c) March



(d) April



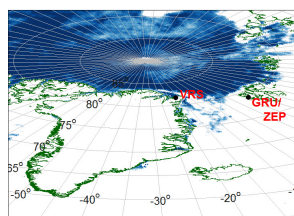
(e) May



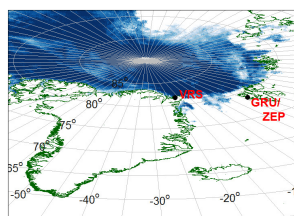
(f) June

8  
9

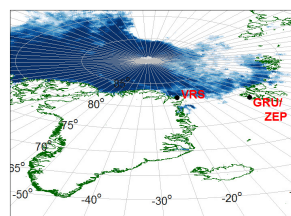
10



(g) July



(h) August



(i) September

11  
12

13

14

15

16

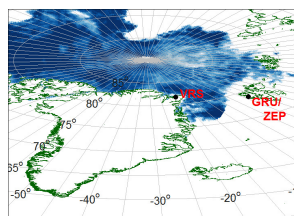
17

18

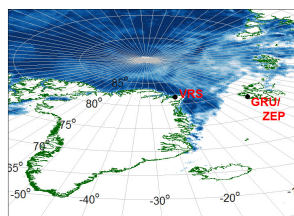
19

20

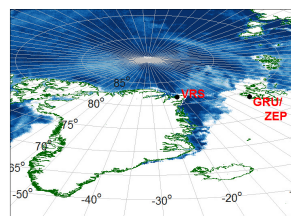
21



(j) October



(k) November



(l) December

**Figure 1b. Sea ice maps (sea ice in dark blue) for the period March-October (a-h). Land borders are marked in dark green. Snow, land and open water in white.**



1  
2  
3  
4  
5  
6  
7  
8  
9  
10  
11  
12  
13  
14

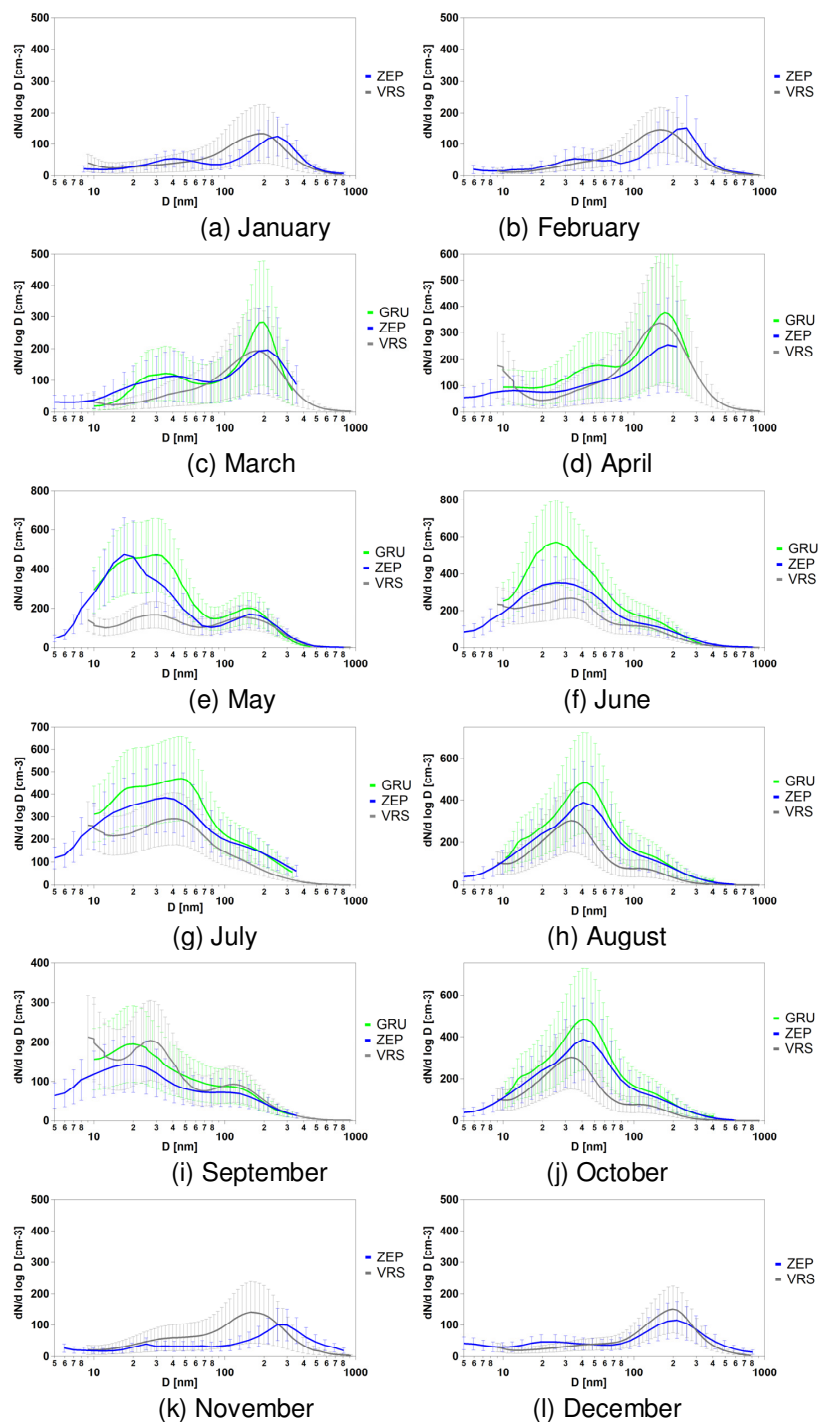
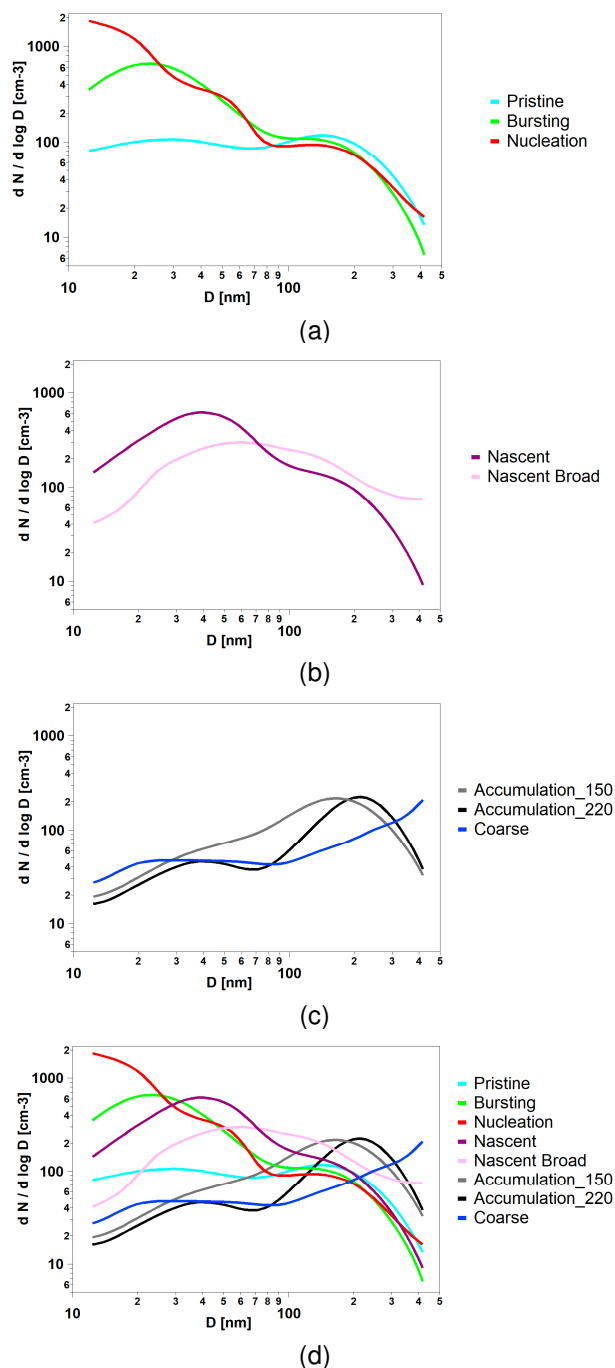


**Figure 2. Monthly average size distributions taken at the three sampling sites for the period January-December (a-l).**



1  
2

3  
4

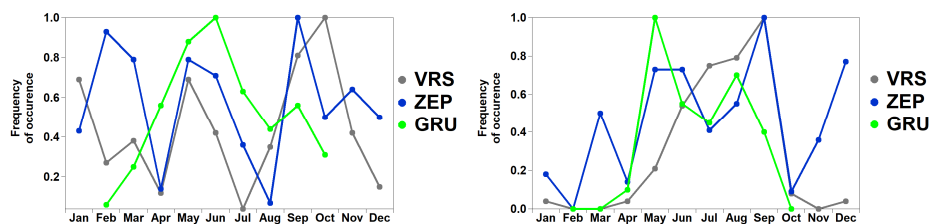
5  
6

7  
8

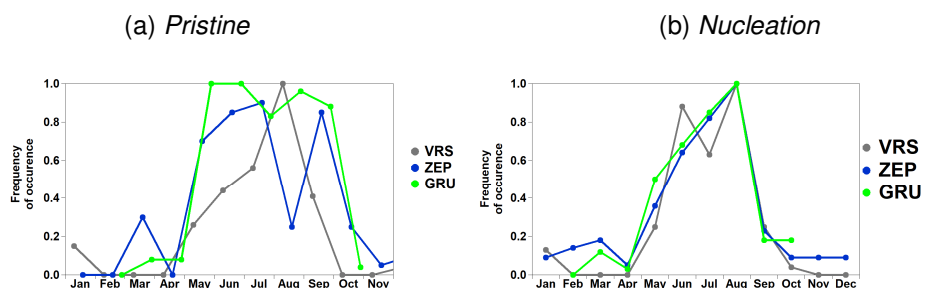
9 **Figure 3. K-means aerosol categories for (a) Pristine, Bursting, Nucleation, (b)**  
 10 **Nascent, Nascent Broad, (c) Accumulation\_150, Accumulation\_220, Coarse, and (d)**  
 11 **all average number aerosol size distributions for each of the three sub-groups.**



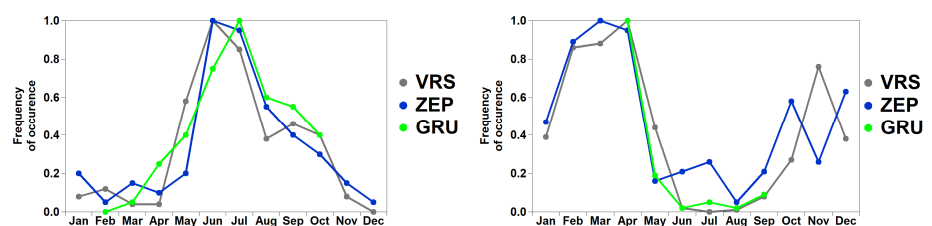
1  
 2



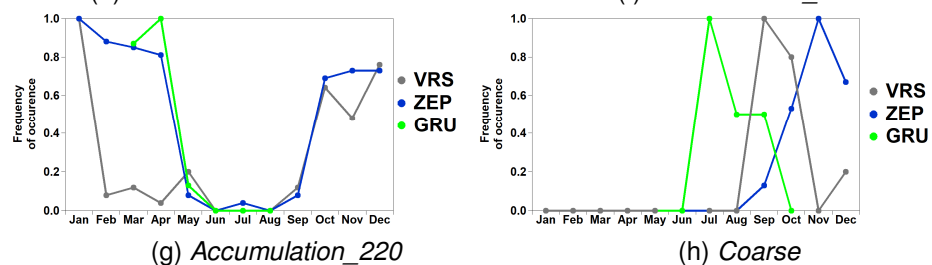
3  
 4  
 5  
 6



7  
 8  
 9  
 10



11  
 12

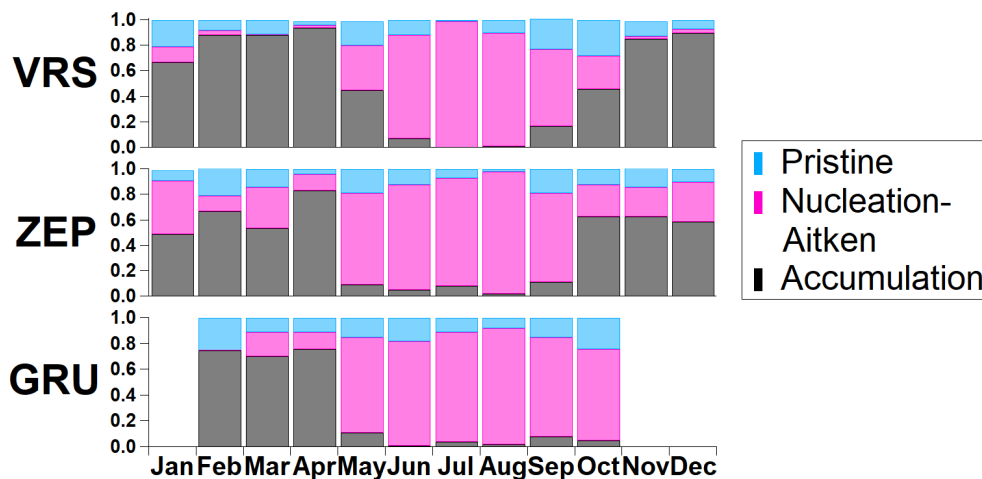


13  
 14  
 15  
 16  
 17  
 18  
 19  
 20  
 21  
 22

**Figure 4. Annual variation of the frequency of the monthly cluster count for the three stations (VSR, ZEP, GRU).**



1  
2  
3  
4  
5

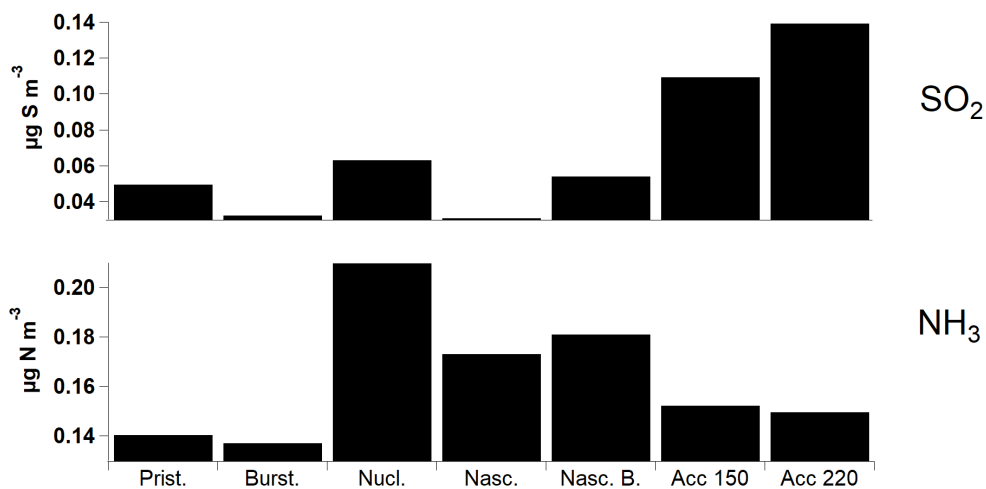


6  
7  
8  
9  
10  
11  
12  
13  
14  
15  
16  
17  
18  
19  
20  
21  
22  
23  
24  
25  
26  
27  
28  
29  
30  
31  
32  
33

Figure 5. Annual variation of the frequency of the monthly cluster count for the three stations (VRS, ZEP, GRU) summarized in sub-aerosol main categories.



1  
2  
3  
4  
5  
6  
7  
8



9  
10  
11  
12  
13  
14  
15  
16  
17  
18  
19  
20  
21  
22  
23  
24  
25  
26  
27  
28  
29  
30  
31  
32  
33

**Figure 6. Average daily concentrations of selected chemical tracers for each aerosol category (ZEP only).**



1  
 2  
 3  
 4  
 5  
 6  
 7  
 8  
 9  
 10  
 11  
 12  
 13  
 14  
 15  
 16  
 17  
 18  
 19

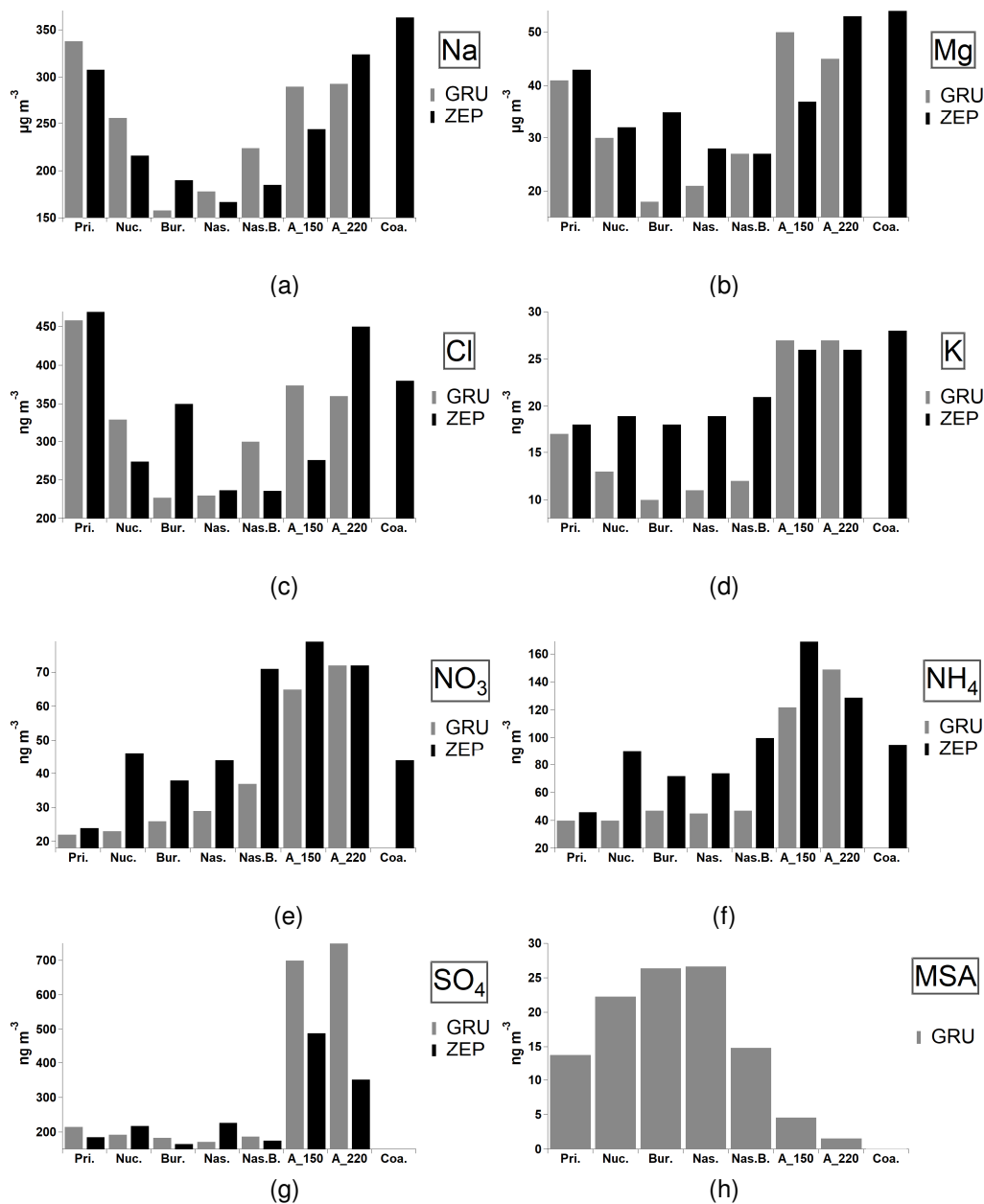
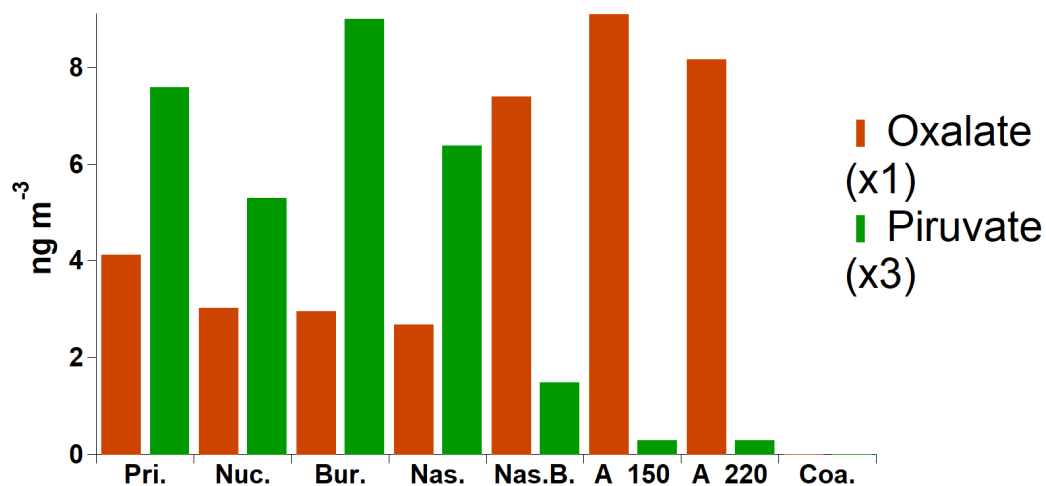


Figure 7. Average daily concentrations of selected chemical tracers for each aerosol category (ZEP and GRU only).



1  
2  
3  
4  
5  
6

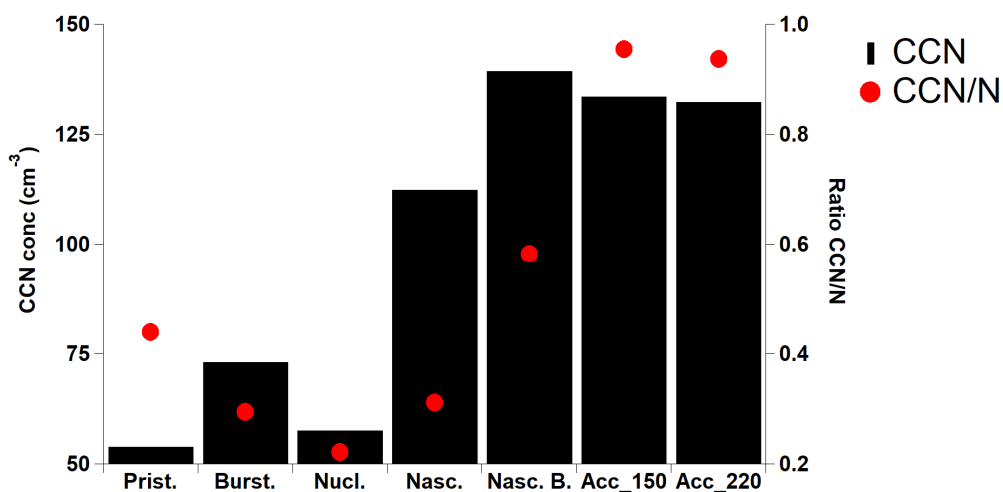


7  
8  
9  
10  
11  
12  
13  
14  
15  
16  
17  
18  
19  
20  
21  
22  
23  
24  
25  
26  
27  
28  
29  
30  
31  
32  
33

**Figure 8. Average daily concentrations of selected chemical tracers for each aerosol category (GRU only).**



1  
2  
3  
4  
5  
6  
7  
8  
9



10  
11  
12  
13  
14  
15  
16  
17  
18

**Figure 9. Average daily concentrations of CCN concentrations for each aerosol category (ZEP only).**